Journal of Inflammation Research

Dovepress
open access to scientific and medical research

Open Access Full Text Article

ORIGINAL RESEARCH

Calcio-Herbal Medicine Divya-Swasari-Vati Ameliorates SARS-CoV-2 Spike Protein-Induced Pathological Features and Inflammation in Humanized Zebrafish Model by Moderating IL-6 and TNF-α Cytokines

This article was published in the following Dove Press journal:
Journal of Inflammation Research

Acharya Balkrishna[1,2]
Sudeep Verma[1]
Siva Kumar Solleti[1]
Lakshmipathi Khandrika[1]
Anurag Varshney[1,2]

[1]Drug Discovery and Development Division, Patanjali Research Institute, Haridwar, Uttarakhand 249 405, India; [2]Department of Allied and Applied Sciences, University of Patanjali, Haridwar, Uttarakhand 249 405, India

Video abstract

Point your SmartPhone at the code above. If you have a QR code reader the video abstract will appear. Or use: https://youtu.be/dylNo-Ayjlg

Purpose: Severe acute respiratory syndrome-coronavirus-2 (SARS-CoV-2) infection has grown into a pandemic and without a specific cure, disease management is the need of the hour through symptomatic interventions. Studies with severe acute respiratory syndrome-coronavirus (SARS-CoV) have highlighted the role of herbal medicines either in combination with antiviral drugs or by themselves in curtailing the severity of infection and associated inflammation. Divya-Swasari-Vati is an Indian ayurvedic formulation used in the treatment of chronic cough and lung inflammation, which is one of the first symptoms of SARS-CoV-2 infections.

Methods: In this study, we used a A549 cell xenotransplant in the swim bladder of zebrafish and modeled the SARS-CoV-2 infection by injecting the fish with a recombinant spike protein. The different groups were given normal feed or feed mixed with either dexamethasone (as the control drug) or Divya-Swasari-Vati. The changes in behavioral fever, infiltration of pro-inflammatory cells in the swim bladder, degeneration or presence of necrotic cells in the kidney, and gene expression of pro-inflammatory cytokines were studied to determine the rescue of the diseased phenotype.

Results: Challenge with the spike protein caused changes in the swim bladder cytology with infiltrating pro-inflammatory cells, skin hemorrhage, and increase in behavioral fever. This was also accompanied by increased mortality of the disease control fish. Treatment with Divya-Swasari-Vati reversed most of the disease symptoms including damage to the kidney glomerulocytes, and complete reversal of behavioral fever. Dexamethasone, used as a comparator, was only able to partly rescue the behavioral fever phenotype. Divya-Swasari-Vati also suppressed the pro-inflammatory cytokines, IL-6 and TNF-α, levels in a dose-dependent manner, under in vivo and in vitro conditions.

Conclusion: The study showed that the A549 xenotransplanted zebrafish injected with the recombinant spike protein of SARS-CoV-2 is an efficient model for the disease; and treatment with Divya-Swasari-Vati medicine rescued most of the inflammatory damage caused by the viral spike protein while increasing survival of the experimental fish.

Keywords: zebrafish, A549 xenotransplant, SARS-CoV-2 infection model, herbal medicines, ayurveda, Divya-Swasari-Vati, behavioral fever, cytokine profile

Introduction

Severe acute respiratory syndrome (SARS) caused by the coronavirus 2019 (SARS-CoV-2) has caused untold morbidity and mortality worldwide. Due to the novel

Correspondence: Anurag Varshney
Tel +91-1334-244107, Ext: 7458
Email anurag@prft.co.in

submit your manuscript | www.dovepress.com
DovePress
http://doi.org/10.2147/JIR.S286199

genomic profile of the virus, current medications have been unsatisfactory in the treatment of the SARS-CoV-2 viral pathology and so far no drugs or therapies have been approved by the FDA.[1] The current modality is to treat the symptoms in an effort to manage the low oxygen concentration in the body and to prevent other incidental infections and co-morbidities such as Diabetes, Heart diseases, and gastro-intestinal problems. Though the actual biology of the infection has been deciphered, treatment still remains elusive, prompting multiple avenues of research being tried out including several traditional remedies.[2,3]

The ayurvedic system of medicine is known to treat the body as a whole rather than the symptoms of the disease and therefore may play a very important role in combating the SARS-CoV-2. The main symptom of an infection with coronavirus is sudden breathlessness due to damage to the alveolar epithelial cells of the lungs. Acute respiratory distress due to acute lung injury by the viral infection can trigger a cascade of immune responses within the pulmonary alveoli. The host immune system is hyperactive during SARS-CoV-2 infection and can result in a sudden increase in several pro-inflammatory cytokines including IL-6, IL-1, TNF-α, and interferons.[4,5] This "Cytokine Storm" can lead to the infiltration of a multitude of immune cells, neutrophils, macrophages, and T cells from the circulation. Neutrophilic infiltration in the pulmonary alveoli can cause the release of granule proteins and reactive oxygen species.[6] Though the exact mechanism of acute respiratory distress is not known in the SARS-CoV-2 infection, the infiltration of these immune cells can lead to a destabilization of the cell-to-cell interactions, damage to vascular barrier, edema, and diffuse alveolar damage.[7–9]

The presence of several diverse phyto-compounds in herbal remedies and other naturally available materials can often lead to a cumulative effect in treating the disease symptoms, and many times with much fewer side-effects. Traditional medicines were successfully used for the treatment of SARS-CoV-2 associated pneumonia like symptoms. Studies have suggested a combination of both the traditional medicine and modern approaches for treatment of this disease and several paradigms are being trialed for decreasing viral load in patients.[10] A group of experts from the Wuhan University Zhongnan Hospital included the use of traditional medicines in the guidelines for the treatment and prevention of SARS-CoV-2, based on their demonstrated efficacy against SARS-CoV.[11] Several herbal mixtures are being tried as ACE-2 blockers, and those that target TMPRSS2, and Papain like proteinase (Plpro) in addition to the remedies that have been used for alleviation of common cold, chronic cough, and asthma.[12]

In this study, we used the herbal formulation Divya-Swasari-Vati (DSV), as a potential treatment option in a SARS-CoV-2 infection model. The formulation (Table 1) is a calcium rich herbal mixture and has been prescribed in chronic cough, common cold, asthma, and phlegm accumulation in the chest in Ayurvedic system of medicine. The herbal components include rare herbs like Salt cresse (Rudanti) and Gall plant (Kakdasinghi), and other commonly found such as the liquorice plant (*Glycyrrhiza glabra*) which is used as a harmonizing agent in several formulations as well as an ayurvedic treatment for many diseases, dried ginger (*Zingiber officinale*), black pepper (*Piper nigrum*), and Indian long pepper (*Piper longum*). Many of these have a long history of being used in treatment of respiratory infections and bronchitis.[13]

SARS-CoV-2 virus is speculated to have originated in bats and been transmitted to humans either directly or indirectly thorough a reservoir host. Though the particular reservoir has not been identified, several species like civets, pangolins, and a few cat species were thought to be involved. A study by Oreshkova et al[14] reported the isolation of SARS-CoV-2 virus from Mink, while artificial intelligence based studies showed a close infectivity pattern of several Mink viruses with SARS-CoV-2.[15] Modeling the disease in common laboratory animals may involve the use of genetically modified rodents that express human ACE-2 protein (either by adenoviral or CRISPR systems), or the use of a mouse adapted virus.[16] These processes are limited by ethical considerations and are time-consuming to establish.

The humanized zebrafish (*Danio rerio*) model was used to study the effects of induction with a recombinant spike protein from SARS-CoV-2, and its effects on overall morphology and cytology of zebrafish swim bladder and kidney. Changes in the pro-inflammatory cytokine gene expression was determined semi-quantitatively in vivo and was replicated in vitro using A549 cells. The air filled swim-bladder of zebrafish has been used as a model for acute lung injury and forms an easy to handle model[17] and it is well documented that a number of viruses such as Sindbis, Chikungunya,[18] and Influenza A[19] in addition to several airborne bacteria and fungi colonize zebrafish.[20] The zebrafish model has a close similarity with the processes that are involved in the progression of a viral infection in humans including the different signaling pathways,

Table 1 Composition of Divya-Swasari-Vati Medicinal Formulation. In Addition, Gum Acacia (*Acacia arabica*) 25 mg, Hydrated Magnesium Silicate 7.5 mg, and Colloidal Silicon Dioxide Have Been Added as the Excipients

Component	Ingredient	Weight
Mulethi (*Glycyrrhiza glabra*)	Root	64 mg
Kakadasingi (*Pistacia integerrima*)	Gall	63 mg
Rudanti (*Cressa cretica*)	Fruit	63 mg
Sounth (*Zingiber officinale*)	Rhizome	42 mg
Chhoti Pipal (*Piper longum*)	Fruit	42 mg
Marich (*Piper nigrum*)	Fruit	42 mg
Dalchini *(Cinnamomum zylancium*)	Bark	32 mg
Akarkara (*Anacyclus pyrethrum*)	Root	32 mg
Lavang (*Syzygium aromaticum*)	Flower bud	32 mg
Mukta-Shukti Bhasma	Herbally processed ash from calcined shell of Pearl oyster (*Pinctada fucata*)	12.6 mg
Abhrak Bhasma	Herbally processed ash from calcined mica	12.6 mg
Kapardak Bhasma	Herbally processed ash from calcined cowry shell of *Cypraea moneta.*	12.6 mg
Godanti Bhasma	Herbally processed ash from rich gypsum	12.6 mg
Sphatika Bhasma	Herbally processed ash from calcined form of alum	12.6 mg
Praval Pishti	Coral calcium powder processed with rose water	12.6 mg
Tankan Bhasma	Herbally processed ash from calcined borax	12.6 mg

chemical interactions, and other physical forces.[21] Xenotransplanted A549 cells in the swim bladder of zebrafish is an accepted model and has a very high success rate in cell transplantation and establishing an in vivo model for several human lung cancers.[22,23]

Materials and Methods

Chemicals and Reagents

All chemicals and reagents used in the study were of the highest commercial grade. SARS-CoV-2 Spike protein (SARS-CoV-2-S) was procured from Bioss Antibodies (Woburn, MA, USA). The Divya-Swasari-Vati tablets were sourced from Divya Pharmacy, Haridwar, India (Batch number #B SWV117). The different components of this medicinal formulation, per tablet, are given in Table 1.

Zebrafish Maintenance

Wild-Type adult zebrafish (*Danio rerio*) were reared in standard experimental conditions in fresh water maintained at 27±1ºC with a 14L:10D photoperiod.[24] Fish were fed in a diurnal cycle with 5 mg per gram body weight using commercially available feed (TetraBit, Spectrum Brands Pet LLC, Blacksburg, VA, USA). Water quality and housing standards were maintained according to Good Animal Practice as per Institutional Animal Ethics Committee in accordance with the Committee for the Purpose of Control and Supervision of Experiments (CPCSEA), India. The study plan was reviewed and approved by the Institutional Ethics Committee, Pentagrit Private Limited, Chennai, Tamil Nadu, India (vide approval number 223/Go062020/IAEC).

A total of 168 fish were used in seven groups with 24 fish each. Two dosing time points were selected, 3 days and 6 days post-induction of pathology using the SARS-CoV-2 spike protein. A schematic of the study is represented in Figure 1, and the characteristics of the fish used for the study are described in Table 2.

Cell Line and Cell Culture

The human lung alveolar epithelial cell line A549 was procured from ATCC licensed repository, National Centre for Cell Sciences (Pune, Maharashtra, India) and was maintained in Dulbecco's Modified Eagle Medium with 10% FBS and 1% antibiotic solution and cultured at 37° C under 5% humidity. The initial stock was passaged thrice, and the third passage was used for the study. For in vitro experiments, cells that are at least 70% confluent were used.

Establishment of Xenotransplant and Induction of SARS-CoV-2 Infection Model

The xenotransplant model was established in 144 fish for each time point, by injecting A549 cells into the posterior lobe of the swim bladder. A549 cells, at a concentration of $2x10^2$ in minimal volume of PBS, were injected

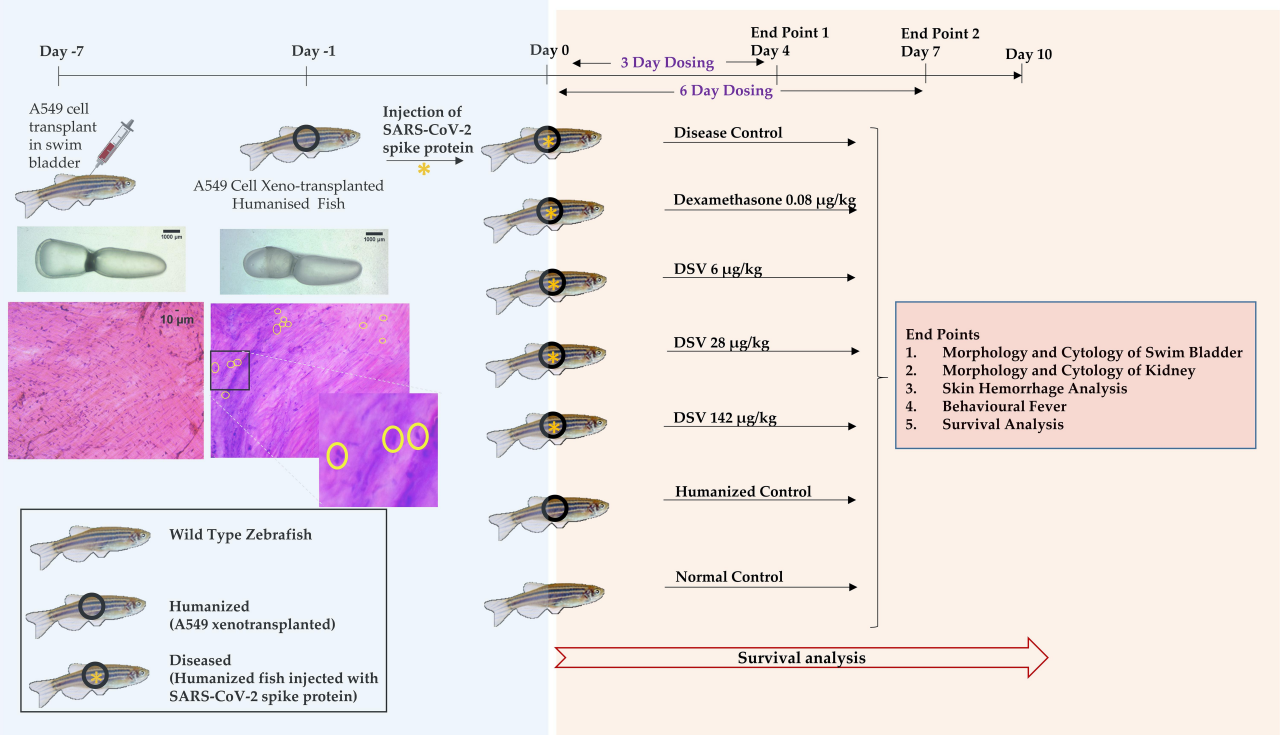

Figure 1 Schematic representing the study design for use of Divya-Swasari-Vati (DSV) as a therapeutic against SARS-CoV-2 in a humanized zebrafish model. Treatment end points were studied for 4 and 7 days. A parallel experiment was also setup to study the survival of the different groups for 10 days. Transplanted A549 cells in the swim bladder are highlighted by yellow circles and shown as a magnified image.

intramuscularly at the junction of the trunk and caudal region, along the midline.[25] Post-injection, the fish were transferred to the respective clutches at 27°C±1°C and were observed for a period of 7 days. Cytology of the swim bladder in a few test fish was studied to confirm the adherence of the human cells to the zebrafish swim bladder epithelium.

Recombinant SARS-CoV-2 spike protein stock was prepared by dissolving 100 µg of the protein in PBS to get a concentration of 1 µg/µL. This was further diluted to a concentration of 1 ng/µL by dissolving 1 µL of the stock (1 µg) in 1 mL PBS. The concentration of the spike protein to induce symptoms of infection was titrated from Coleman et al[26] based on their studies in mice. Post the 7-day period and after confirmation of a successful xenotransplantation, 2.8 ng protein was injected carefully at the site of transplantation.

Table 2 General Characteristics of Zebrafish Used in the Study

Criteria for Selection of Zebrafish	
Gender	Male and Female
Age	1 Year
Body weight	0.5 gm
Body length	25 to 30 mm
No. of fish per group	24
No. of fish per clutch	12
Tank capacity	6 liters

To prepare the fish for injection, hypothermia was used as an anesthetic. The anesthesia tank was set with two adjacent baths maintained at 17°C and 12°C. Each fish was gently transferred from the respective clutches to the 17°C tank and was in the tank until a decrease in the operculum movement was observed. After this, the fish was transferred to the 12°C tank until there was no response to caudal fin touch. Each of the anesthetized fish was placed on to the injection stage and the SARS-CoV-2 recombinant protein was injected at the desired concentration to the posterior lobe of the swim bladder. After the spike protein injection, the fish were maintained at 27±1°C to aid in the stabilization of any physiological and immunological changes.

Oral Dosing

The equivalent dose for the zebrafish was translated from the human dose by body weight. The reference compound (dexamethasone) was given at a single dose while the test formulation (DSV) was used at three dilutions, 0.2X, 1X,

and 5X, as described in Table 3. For infusing the fish feed, the required amount of the compound or formulation was mixed with the feed based on the amount of 2.5 mg feed per pellet. The spiked feed was extruded into uniform pellets and fed to the fish in a 24-hour cycle with the required number of pellets per fish.

The dosing was performed on each fish isolated in a feeding tank separately. Control fish were fed with the unmodified fish feed and were fed under the same conditions as that of the study groups. The dosing was done for two different time points, 3 days and 6 days, to study the acute and sub-acute pathophysiological changes as a result of the SARS-CoV-2 spike protein challenge and treatment with either the reference or test compounds. The fish were sacrificed on day 4 or day 7 for the analysis.

Physiological and Anatomical Observations

Dissection of Swim Bladder for Anatomical and Cytological Observations

Fish were euthanized in water at 2–4°C and dissected as per ethical norms. Each fish was dissected through a ventral incision in the skin from the lower jaw to the vent. The intestinal tract and gonads were removed to expose the swim bladder located ventral to the kidney. This was isolated without any damage to the connected esophagus. The swim bladder was washed repeatedly in PBS and observed under a CZM4 stereomicroscope (Labomed, Los Angeles, CA, USA) at 1X magnification and recorded using a 14 MP camera for anatomical changes. The whole swim bladder was mounted on glass slides for cytological examination and stained with Hematoxylin and Eosin staining.

Dissection of Kidney for Anatomical and Cytological Observations

Euthanization and dissection of the fish were performed as above. For harvesting the kidney, the fish was pinned with the ventral side up and the heart, intestinal cavity, and gonads were removed to expose the kidney attached to the dorsal body wall. Anatomical recording was done using a CZM4 stereomicroscope and recorded as described earlier. Whole kidney was mounted on a glass slide for cytological examination and stained with Hematoxylin and Eosin.

Screening for Skin Hemorrhage

Whole animal imaging was performed using a digital single lens reflex (D3100, Nikon Corporation, Tokyo, Japan) camera for demarking the features that represent the presence of hemorrhagic spots on the skin. Fish were euthanized and were imaged on a glass slide. The area of hemorrhage was measured using calipers and was documented as mm^2.

Behavioral Fever

Direct measurement of body temperature is not feasible in an ectothermic animal like zebrafish. An alternate method is to observe its behavior in water at different temperatures as a measure of its body temperature. An experimental tank was set up with three interconnected chambers and each chamber was maintained at a constant water temperature of 23°C, 29°C, and 37°C. The tank is supplied with continuous heating or cooling to maintain the desired temperature throughout the experimental period. Each fish was introduced to the temperature gradient chamber at 29°C, thereby giving the fish the means to migrate to a chamber that supports its body temperature. The time spent by the fish in each chamber was measured for a 3 minute period.

Survival Analysis by Kaplan–Meier Curve

Mortality of fish was counted on a daily basis to determine the survival, and to plot the K-M curves of the study groups with the different therapeutic interventions.

Semi-Quantitative Gene Expression Analysis for IL-6, IL-10, and TNF-α

Total RNA from peripheral blood was extracted by employing QIAamp RNA Blood Mini Kit (Qiagen, Hilden, Germany)

Table 3 Oral Dosage of Divya-Swasari-Vati and Dexamethasone Used in the Study

Dexamethasone		**Divya-Swasari-Vati (DSV)**		
			per Fish (0.5 gm)	**per kg (Body weight)**
Human Dose	6 mg per day	Human Dose	2 gm per day	
Translational Dose	0.04 ng/fish (0.08 µg/kg)	Translational Dose (0.2X)	3 ng	6 µg/kg
		Translational Dose (1X)	14 ng	28 µg/kg
		Translational Dose (5X)	71 ng	142 µg/kg

following manufacturer's instructions. DNase (New England Biolabs, Ipswich, MA, USA) treatment was performed to remove any DNA material. RNA concentrations were determined by measuring the optical density at 260-nm wavelength followed by an evaluation for protein contamination by ensuring that the ratios for read out at 260/280 nm were maintained between 1.8–2.0. cDNA synthesis was carried out from 1 µg of total RNA using oligo (dT) priming and SuperScript II reverse transcriptase (Invitrogen, Carlsbad, CA, USA) following manufacturer's protocol. The final reaction volume was set at 20 µL for reverse transcription. PCR reactions were carried out using REDTaq® ReadyMix™ PCR Reaction Mix (Sigma Aldrich, St. Louis, MI, USA) following manufacturers protocols for 30–40 cycles using Applied Biosystems GeneAmp PCR System 9700 (Foster City, CA, USA). Primers used for the IL-6 amplification (Forward 5′-ATGCCATCCGCTCAGAAAACAG-3′ and reverse 5′-CCAAGGAGACTCTTTACGTCCA-3′), for IL-10 amplification (Forward 5′-AAGCGGGATATGGTGAAATG-3′ and reverse 5′- CCCCCTTTTCCTTCATCTTT-3′), and for TNF-α amplification (Forward 5′-AGGCAATTTCACTTCCAAGG-3′ and reverse 5′-AGGTCTTTGATTCAGAGTTGTATCC-3′). The amplicons were resolved using agarose gel electrophoresis, and fluorescence was quantified by ImageJ software from National Institutes of Health (Bethesda, MD, USA).

A549 Cell Viability Assay

The cell viability assay was performed under standard conditions using Alamar Blue reagent (HiMedia Laboratories Pvt. Ltd., Mumbai, Maharashtra, India). In brief, $3x10^4$ cells were seeded in a 96 well plate, in triplicate, and incubated in the presence of different concentrations of Divya-Swasari-Vati (0.1, 0.3, 1, 3, 10, 30 and 100 µg/mL) for a period of 24 hours. Two hours before termination, 10 µL of Alamar Blue (0.15 mg/mL) was added to each well and the cell cytotoxicity was measured at an emission of 590 nm with 540 nm excitation, using an Envision microplate reader (PerkinElmer, Waltham, MA, USA).

In vitro Quantification of Cytokines IL-6 and TNF-α Post IL-1β Stimulation in the Presence of Divya-Swasari-Vati

A549 cells were pretreated with different concentrations of Divya-Swasari-Vati as above, for 24 hours and for 72 hours. This was followed by co-treatment with 500 pg/mL human IL-1β and Divya-Swasari-Vati for a further 24 hours. Cell culture supernatant was collected and used for ELISA (BD Biosciences, San Jose, CA, USA), according to the manufacturer's instructions. The absorbance was measured at 450 nm using an Envision microplate reader (PerkinElmer, Waltham, MA, USA).

Data Analysis and Statistics

Data is displayed graphically as a mean±standard deviation (SD) for all experiments using the GraphPad Prism 7.04 software (San Diego, CA, USA). Two-way ANOVA with post-hoc Tukey's test was used to compare significance of data and a *P*-value less than 0.05 was considered significant.

Determination of Phytocompounds Present in Divya-Swasari-Vati Formulation

Experimental Methods

Analysis was performed by HPLC (Waters Corporation, USA) equipped with Binary pump (1525), PDAD (2998), and Auto-sampler (2707). Separation was achieved using a Shodex C18-4E (5 µm, 4.6x250 mm) column subjected to binary gradient elution. Two solvents were used for the analysis and consisted of water containing 0.1% orthophosphoric acid, adjusted to pH 2.5 with diethylamine (solvent A), and 0.1% orthophosphoric acid in a mixture of acetonitrile and water in the ratio 88:12, adjusted to pH 2.5 with diethylamine (solvent B). Gradient programming of the solvent system was initially at 95–90% A for 0–10 minutes, 90–65% A from 10–30 minutes, 65–50% A from 30–40 minutes, 50–25% A from 40–50 minutes, 25% A from 50–55 minutes, 25–15% A from 55–65 minutes, 15–95% A from 65–66 minutes, and 95% A from 66–70 minutes, with a flow rate of 1.0 mL/min. Then 10 µL of standard and test solution was injected and the column temperature was maintained at 35°C. Wavelengths were set at 250 nm (for Ellagic acid and Glycyrrhizin) and 278 nm (for Gallic acid, Protocatechuic acid, Methyl gallate, Coumarin, Cinnamic acid, Eugenol, 6-Gingerol, Piperine, and Glabridin).

Sample Preparation

A 0.5 gm powdered Divya-Swasari-Vati sample was diluted with 10 mL of methanol:water (80:20) and sonicated for 30 minutes, centrifuged at 10,000 rpm for 5 minutes, and filtered using 0.45 µm nylon filter. The standard compounds: Gallic acid was purchased from Loba Chemie (Mumbai, Maharashtra, India); Ellagic acid, Piperine, Eugenol, Glycyrrhizin, Coumarin from Sigma-Aldrich (St. Louis,

MO, USA); Protocatechuic acid, Glabridin from Natural Remedies (Greater Noida, Uttar Pradesh, India), Methyl gallate from Tokyo Chemical Industry (Tokyo, Japan), 6-Gingerol from Cayman Chemical (Ann Arbor, MI, USA), and Cinnamic acid from Sisco Research Laboratories (Mumbai, Maharashtra, India). Standards were dissolved in methanol to prepare the appropriate concentrations.

Results

Divya-Swasari-Vati Reverses the Edema Observed in the Swim Bladder Upon Challenge with SARS-CoV-2 Recombinant Spike Protein

The Zebrafish swim bladder is a gas filled chamber that is two lobed, an anterior and a posterior lobe, connected by a wide ductus communicans. The inner gas gland is made of mesothelium comprising of epithelial cells and smooth muscle musculature, and is covered by tunica externa. The posterior lobe is connected to the esophagus via the pneumatic duct; both the anterior and posterior lobes work in synchrony.

After 7 days of xenotransplant with A549 cells in the air bladder of zebrafish (HZF), both the lobes of the air bladder show normal size, shape, and color with continuous tunica externa and mesothelium lining of smooth muscle, similar to that seen in the control fish (Figure 2). In contrast, the air bladder isolated from the xenotransplanted fish spiked with recombinant SARS-CoV-2 Spike protein (HZF-CoV-2-S) showed an air bladder that was structurally abnormal, being inflated in the anterior lobe, suggesting edema. The fish treated with dexamethasone (0.08 µg/kg body weight), appeared to have a mildly inflated swim bladder with intact tunica externa and gas gland. Swim bladders from fish treated with Divya-Swasari-Vati for 3 days post-spike protein injection did not show any changes in morphology, as compared to normal. DSV treatment of 6 µg/kg body weight, 28 µg/kg, or 142 µg/kg body weight showed normal inflation of both the chambers based on size, shape, or color when compared to the control.

The humanized zebrafish with the spike protein (disease control) had a more drastic structural change in the swim bladder with 6 day induction. The anterior lobe of the bladder was structurally collapsed due to the presence of edematous gas. The group treated with dexamethasone also showed structural anomaly with an enlarged anterior lobe and a narrower posterior lobe due to edematous gas gland. Among the DSV treated fish, the group treated with 6 µg/kg body weight showed structurally collapsed and a slightly reduced inflation of the anterior lobe, indicating that the dosage was not enough. The group treated with 28 µg/kg body weight showed an enlarged anterior lobe indicating edema of the gas gland which appeared to be disfigured. The last group with 142 µg/kg body weight dosage showed recovery of normal features of the swim bladder in terms of size, shape, and color similar to that seen with the control group.

Cytology and Immunological Profile of Swim Bladder After Induction with the SARS-CoV-2 Spike Protein and Treatment with Divya-Swasari-Vati

Cytological examination of the swim bladder after staining with Hematoxylin and Eosin showed nuclear morphology characteristic of the different cells present in the bladder. The different cell types identified in the control fish were, spherical nucleated squamous epithelium, oval nuclei of columnar epithelium, elongated nuclei of smooth muscle, and predominant staining of eosinophilic collagen present prominently in the cytology slide (Figure 3). The xenotransplanted group showed similar cytological features as compared to the control group after 7 days of A549 cell transplantation. Induction of disease phenotype with the Spike protein of SARS-CoV-2, however, showed a heightened immune response with the presence of cellular debris and edema identified by the presence of basophilic nuclear debris and attenuated eosinophilic staining. As a response to the inflammation, the cytological examination showed infiltration of granulocytes and macrophages, as identified by their nuclear morphology (Table 4).

The dexamethasone treated group showed moderate infiltration of granulocytes and lymphocytes with prominent cellular debris indicating rescue from immune response. Fish treated with Divya-Swasari-Vati at dosages of 6 µg/kg and 28 µg/kg body weight showed moderate infiltration of granulocytes and elevated lymphocyte count with normal epithelial and myocyte cytology. Treatment with the DSV dose of 142 µg/kg showed a significant rescue of the disease morphology with reduction of granulocytes which are cellular inflammatory markers. A significantly ($P<0.0001$, compared to the HZF-CoV2-S group) elevated lymphocyte count and reduced cellular debris are clearly seen in the cytology post 3-day treatment (Table 4).

When compared with 3-day induction with the SARS-CoV-2 spike protein, 6-day shows no infiltration of granulocytes, macrophages, or lymphocytes beyond the normal

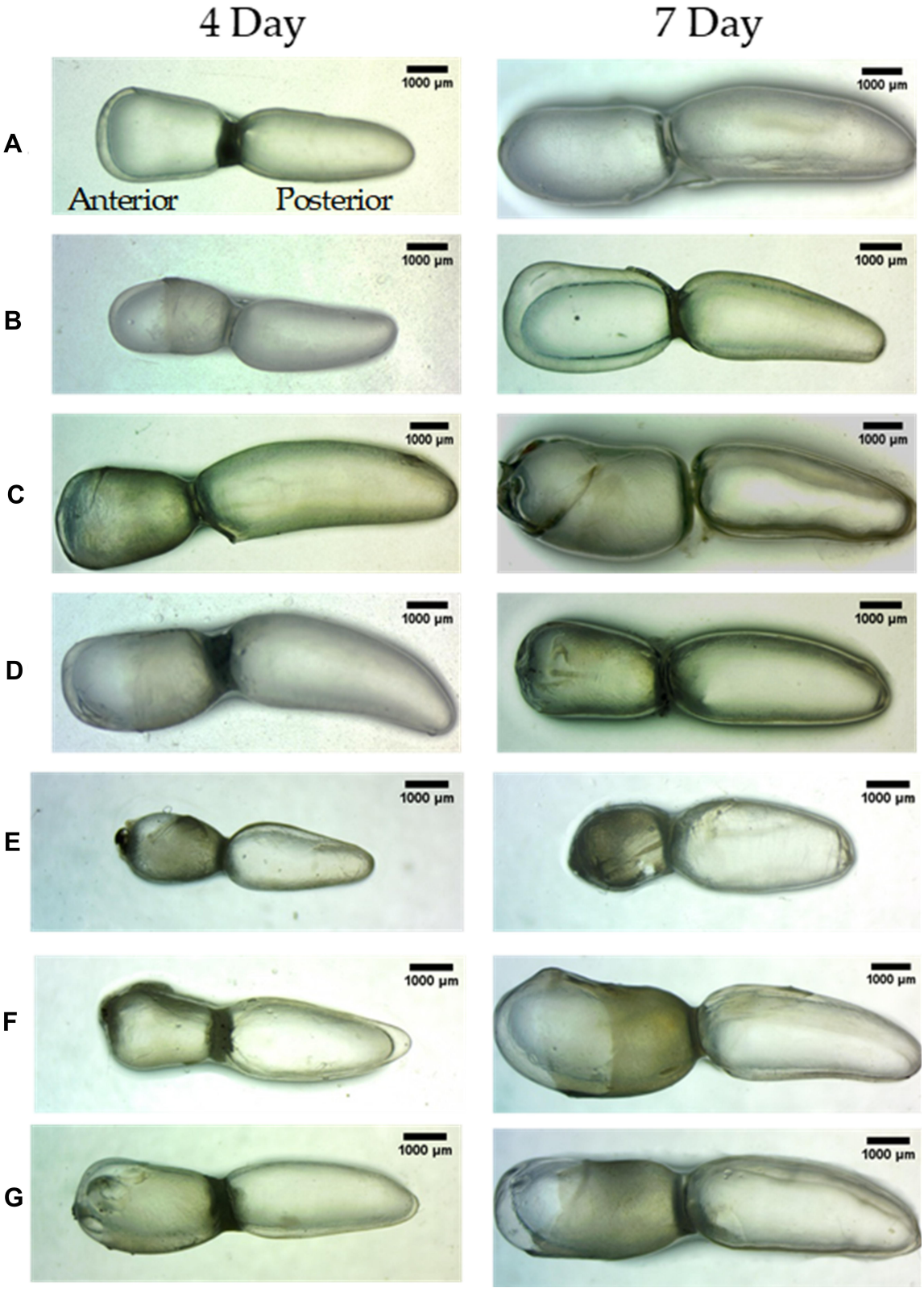

Figure 2 Lateral view of swim bladder with the dorsal region on top and the cranial facing region to the left. The anterior and posterior lobes are labelled. Images were taken at 10X magnification. (**A**) Normal Control (**B**). Humanized Zebrafish with xenotransplanted A549 cells (HZF) (**C**). Diseased fish with SARS-CoV-2 spike protein (HZF-SARS-CoV-2-S) (**D**). Dexamethasone (0.08 µg/kg) treatment (**E**). Divya-Swasari-Vati treatment (6 µg/kg) (**F**). Divya-Swasari-Vati treatment (28 µg/kg) (**G**). Divya-Swasari-Vati treatment (142 µg/kg).

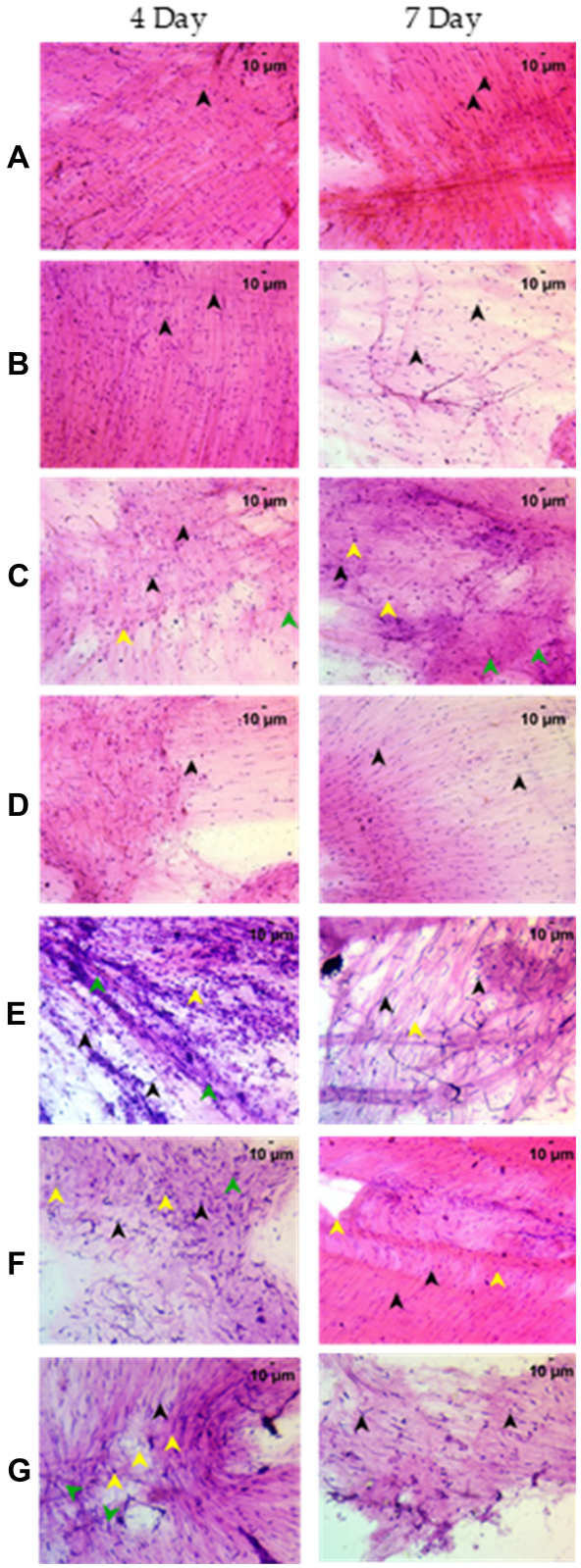

Figure 3 Cytological examination of the whole swim bladder after staining with Hematoxylin and Eosin at 200X magnification. (**A**) Normal Control (**B**). Humanized Zebrafish with xenotransplanted A549 cells (HZF) (**C**). Diseased fish with SARS-CoV-2 spike protein (HZF-SARS-CoV-2-S) (**D**). Dexamethasone (0.08 µg/kg) treatment (**E**). Divya-Swasari-Vati treatment (6 µg/kg) (**F**). Divya-Swasari-Vati treatment (28 µg/kg) (**G**). Divya-Swasari-Vati treatment (142 µg/kg). Black arrowheads depict the nuclei of normal cells. Green arrowheads show granulocytes and the yellow arrowheads show macrophages.

Table 4 Quantification of the Immune Cell Infiltration in the Air Bladder Cytology. Infiltration of Lymphocytes, Macrophages, and Granulocytes Was Quantified on a Hematoxylin and Eosin Stained Air Bladder from Each Fish. The Results are Expressed as Mean ±SD. Statistical Analysis Was Performed Using ANOVA and Significance as Denoted by * $P<0.0001$ When Compared with the HFZ-CoV2-S Group

Study Groups	4 Day			7 Day		
	Granulocyte	Macrophage	Lymphocyte	Granulocyte	Macrophage	Lymphocyte
Control	0	0	0	0	0	0
HZF	0	0	0	0	0	0
HZF-CoV-2-S	11±5.2	7±3.5	0	0	0	0
Dexamethasone	5*±2.9	0*	20*±5.0	0	9*±5.4	10*±6.2
DSV-6 µg/kg	7.08*±4.6	0*	31*±6.6	0	0	23.71*±5.0
DSV-28 µg/kg	5.33*±3.1	0*	53.96*±5.7	0	0	19.17*±6.8
DSV-142 µg/kg	3.42*±3	0*	113.29*±5.5	0	0	16*±6.3

distribution of epithelial cells and myocytes. A heightened inflammatory response was seen due to the presence of basophilic nuclear debris and attenuated eosinophilic stain. The dexamethasone treated group did not show any infiltrating granulocytes but had a significantly ($P<0.0001$) higher number of macrophages and lymphocytes (Table 4). Cytological staining also identified prominent cellular debris that could be a result of rescue from immune response (Figure 3). The Divya-Swasari-Vati treated group showed a gradual dose-dependent rescue of disease markers seen by cytology and a significantly ($P<0.0001$) higher infiltration of lymphocytes but no presence of either macrophages or granulocytes at 6 µg/kg body weight dosage. The group given 28 µg/kg and 142 µg/kg body weight showed well defined epithelial and myocyte count with a significantly increased lymphocyte count. A dose-dependent rescue of disease morphology was evident with no cellular inflammatory markers such as macrophages or leukocytes.

Treatment with Divya-Swasari-Vati Rescued the Vascular Degeneration and Necrosis of the Kidney Upon Induction with SARS-CoV-2 Spike Protein

The zebrafish kidney is divided into the head, saddle or trunk, and a tail extending from the anterior to the posterior of the body. It is located in the dorsal wall of the body cavity attached to the parenchymal liver. Anatomical observation of the kidney from control fish showed well defined internal arrangements where the mesonephric nephrons are packed in the head kidney with glomerular tufts followed by proximal and distal tubule segments. The mesonephros appeared to be highly pigmented with melanocytes and are distributed throughout the kidney from head to tail (Figure 4). Even after 7 days of A549 cell transplant into the air bladder, there was no change in the morphology of the kidney in the HZF group, indicating that there was no deleterious effect of adding the cells to the fish. In contrast, the group of fish with the SARS-CoV-2 spike protein, after 3 days, revealed structural anomalies with the loss of tubular segments and vascular degeneration indicating renal necrosis.

Treatment with dexamethasone showed a slow return to normal morphology with arborized kidney network with packed glomerular tufts and tubular segments indicating normal renal architecture. This was not as prominent as that seen with DSV treatment where all the three dosages showed a packed network of mesonephros with highly pigmented melanocytes that could be seen distributed throughout the kidney indicative of a normal renal morphology.

After 6 days of induction with the spike protein of SARS-CoV-2, structural anomalies were seen with the loss of tubular segments and vascular degeneration indicating renal necrosis. Treatment with dexamethasone did not fully rescue the disease as seen by a disorganized kidney network with irregular glomerular tufts and melanocyte pigmentation, indicators of structural anomaly (Figure 4). Treatment with DSV showed complete rescue of the anatomical changes and a normal renal morphology was observed, with a packed network of mesonephros and highly pigmented melanocytes that are distributed throughout the structure. Such a rescue phenomenon was seen with all the three dosages of DSV formulation tested.

Cytological Examination of the Kidney for Detecting Necrosis

The renal epithelial cells are identified by their tubular structures with hematoxylin and eosin staining of the cytological

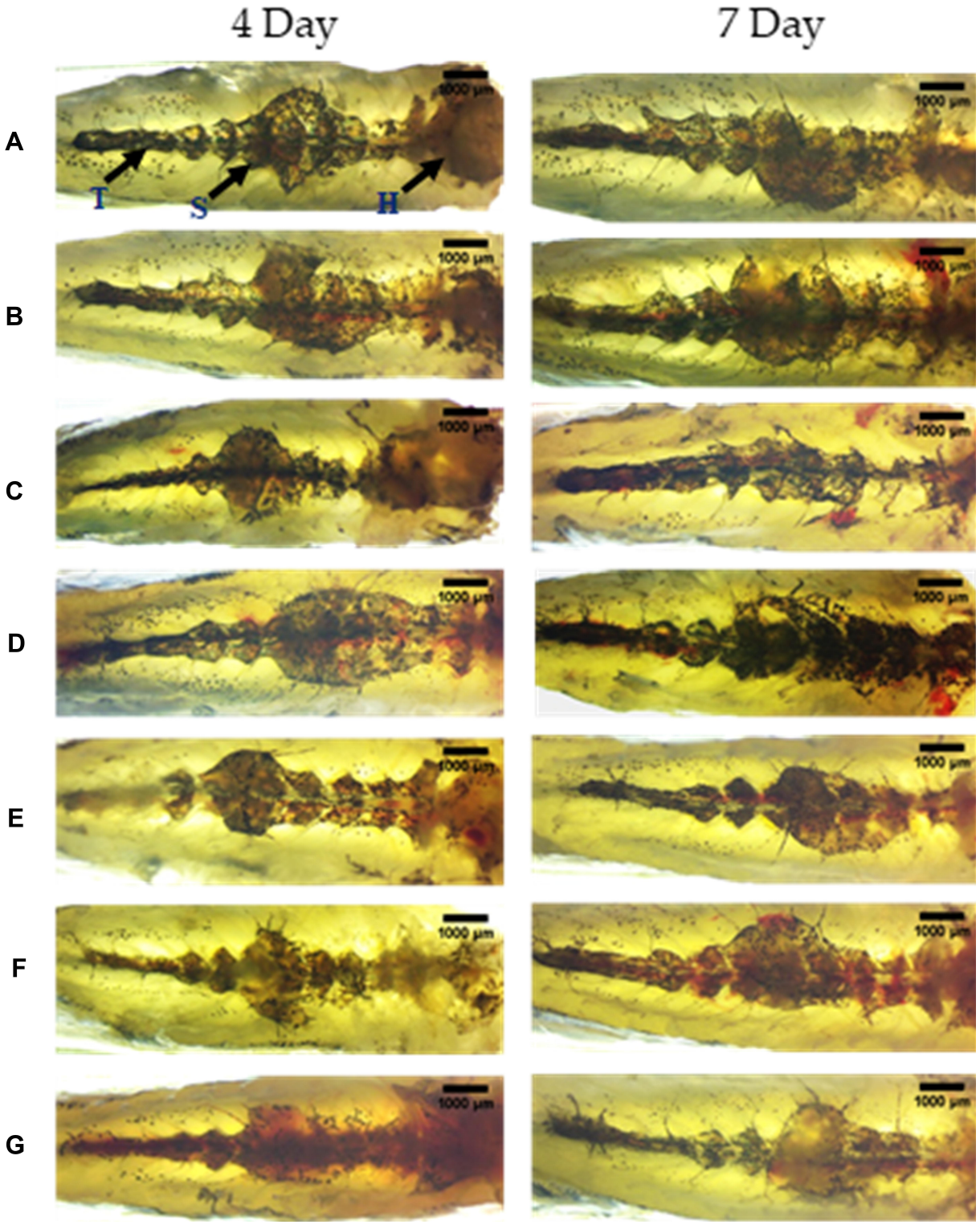

Figure 4 Structural examination of the kidney at 10X magnification. The three regions of the kidney Head (H), Trunk or Saddle (S), and Tail (T) extend from the anterior to the posterior of the body. (**A**) Normal Control (**B**). Humanized Zebrafish with xenotransplanted A549 cells (HZF) (**C**). Diseased fish with SARS-CoV-2 spike protein (HZF-SARS-CoV-2-S) (**D**). Dexamethasone (0.08 µg/kg) treatment (**E**). Divya-Swasari-Vati treatment (6 µg/kg) (**F**). Divya-Swasari-Vati treatment (28 µg/kg) (**G**). Divya-Swasari-Vati treatment (142 µg/kg).

mount of the kidney. The normal control and A549 xenotransplanted group showed arborized tubular network of the mesonephros with evenly scattered erythrocytes and glomerulocytes representing the normal renal pathology (Figure 5). In the HZF-CoV-2-S group, cytological examination showed disorganized cellular arrangement, including

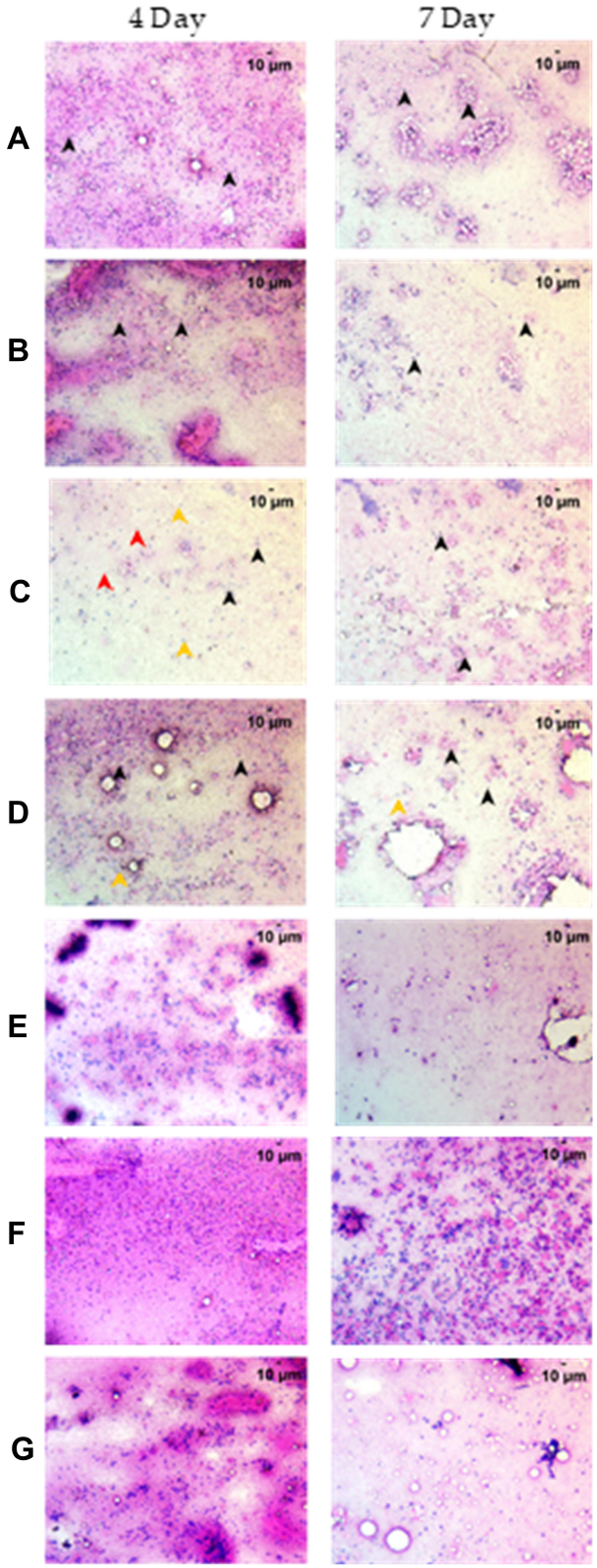

Figure 5 Cytological examination of the kidney after staining with Hematoxylin and Eosin at 200X magnification. (**A**) Normal Control (**B**). Humanized zebrafish with xenotransplanted A549 cells (HZF) (**C**). Diseased fish with SARS-CoV-2 spike protein (HZF-SARS-CoV-2-S) (**D**). Dexamethasone (0.08 µg/kg) treatment (**E**). Divya-Swasari-Vati treatment (6 µg/kg) (**F**). Divya-Swasari-Vati treatment (28 µg/kg) (**G**). Divya-Swasari-Vati treatment (142 µg/kg). Black arrowheads depict the nuclei of normal cells, yellow represent degenerative cells, while the red arrowheads depict necrotic cells.

erythrocyte aggregation, with significantly (P<0.0001) higher degenerative and necrotic epithelial cells (Table 5). The degenerative cells are mostly basophilic with a mildly stained nucleus.

Treatment with dexamethasone (0.08 µg/kg) after 3 days showed normal distribution of erythrocytes (identified by their defined nucleus), epithelial podocytes, and endocrine cells. There was a significant (P<0.0001) reduction in the percentage of degenerative cells and overall necrosis (Table 5). The DSV treated group showed dose-dependent rescue of cytological features. Treatment with 6 µg/kg and 28 µg/kg body weight showed mildly stained basophilic renal epithelial cells with a significantly (P<0.0001) lower percentage of necrotic and degenerative cells. The group treated with 142 µg/kg DSV for 3 days showed the best cytological profile with well-defined erythrocytes and tubular epithelial cells distributed throughout (Figure 5), with very low cellular necrosis and degeneration.

Induction of disease pathology with the recombinant SARS-CoV-2 spike protein showed cytological changes to the kidney with disorganized cellular arrangement after 6 days. Erythrocyte aggregation and a higher percentage of mostly basophilic degenerative and necrotic renal epithelial cells with mildly staining nucleus (Figure 5). Treatment with 0.08 µg/kg body weight dexamethasone showed mildly basophilic epithelial cells and erythrocytes with mildly stained nuclei, suggesting a loss of normal cytological traits. There was a significant (P<0.0001) reduction in the percentage of the degenerative and necrotic cells when compared to the HZF-SARS-CoV-2-S group (Table 5). The DSV treated group showed a gradual dose-dependent rescue of cytological damage. The 6 µg/kg group showed loss of renal epithelial cell architecture with highly distributed necrotic and degenerative cells. When compared to the infected control, the low dose of the test formulation showed a non-significant reduction in the percentage of nephrotic cells and a slightly significant (P<0.05) reduction of degenerative cells. Treatment with 28 µg/kg showed moderately distributed degenerative cells with an aggregated erythrocyte network. There was a significant (P<0.0001) reduction in the percentage of necrotic and degenerative cells. The group treated with 142 µg/kg body weight DSV showed the most recuse phenotype with normal renal epithelial cytology similar to that of the normal control fish, and significantly lower degenerative and necrotic cell percentage.

Induction with the Recombinant Spike Protein of SARS-CoV-2 Causes Skin Hemorrhage That Was Reversed by Treatment with Divya-Swasari-Vati

The presence or absence of hemorrhagic spots under the skin of zebrafish was scored and the total area of the hemorrhagic region was quantified. In contrast to the normal control and the xenotransplanted control fish, the HFZ-CoV-2-S group showed clinical signs of hemorrhaging at the pelvic, anal, dorsal, and caudal fin. Treatment with either dexamethasone or DSV (in three different dosages) reversed the clinical signs of hemorrhaging at the skin after both the time points, 3 and 6 days, used in the study (Figure 6).

The regions of hemorrhage were measured in seven individual fish and the 3-day induction with SARS-CoV-2 spike protein showed an average area of 21.23±0.6 mm^2 which was significantly (P<0.0001) higher than that of the

Table 5 Cytological Profile of the Renal Tissue to Determine Necrotic and Degenerative Cells. Renal Epithelial Cells Were Identified by Their Tubular Morphology in a Hematoxylin and Eosin Stained Slide from Each Fish and the Percentage of Degenerative and Necrotic Cells Was Calculated. The Results are Expressed as Mean±SD and Statistical Analysis Was Preformed Using ANOVA. Significant Differences When Compared with the HFZ-CoV-2-S Group Were Denoted by ** P<0.0001 and by * P<0.05

Study Groups	4 Day		7 Day	
	% Necrosis	% Degenerate Cells	% Necrosis	% Degenerate Cells
Control	0	0	0	0
HZF	0	0	0	0
HZF-CoV-2-S	8.04± 4.7	40±5.9	20.33±6.5	49.54±5.3
Dexamethasone	2.17**±1.7	19.92**±6.0	10.25**±6.5	34.71**±5.8
DSV-6 µg/kg	1.75**±1.2	19.63**±5.2	20.04*±5.4	44.75**±6.6
DSV-28 µg/kg	1.96**±1.2	12.33**±5.5	13.04**±6.9	19.29**±5.8
DSV-142 µg/kg	1.46**±1.0	6.96**±4.7	3.08**±2.3	6.96**±3.5

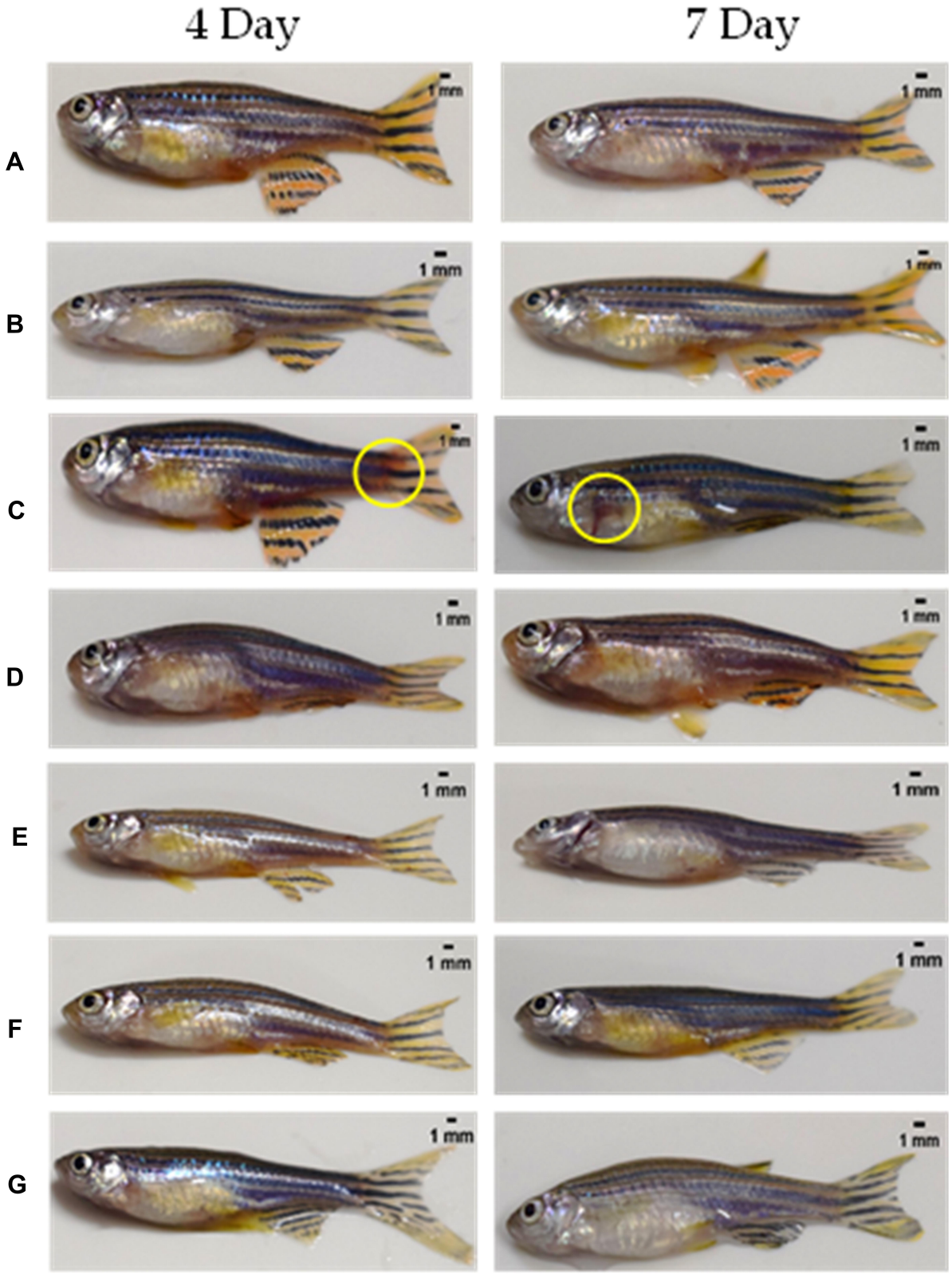

Figure 6 Whole animal imaging for the presence of hemorrhagic regions on the skin. (**A**) Normal Control (**B**). Humanized Zebrafish with xenotransplanted A549 cells (HZF) (**C**). Diseased fish with SARS-CoV-2 spike protein (HZF-SARS-CoV-2-S) (**D**). Dexamethasone (0.08 µg/kg) treatment (**E**). Divya-Swasari-Vati treatment (6 µg/kg) (**F**). Divya-Swasari-Vati treatment (28 µg/kg) (**G**). Divya-Swasari-Vati treatment (142 µg/kg).

HZF control and the normal control group which did not show any signs of hemorrhage. The average area of skin hemorrhage after 6-day induction was slightly lower at 9.43±0.6 mm^2 and was still significantly higher than the control groups. Treatment with dexamethasone or with the three different dosages of DSV ameliorated the skin hemorrhage and the appearance of the fish was similar to the normal controls.

Divya-Swasari-Vati Rescues Behavioral Fever Phenotype Post Induction with Spike Protein of SARS-CoV-2

Behavioral fever is a synergic response to infection in zebrafish where the fish move to regions that are having the same temperature as that of their body during the fever associated with an infection. It was observed that the normal control and the xenotransplanted control group (HZF) spent more time in the temperature chamber at 29°C indicating healthy individuals without any behavioral fever. The fish with the recombinant spike protein of SARS-CoV-2 (HZF-SARS-CoV-2-S) spent more time in the chamber at 37°C indicating changed behavior due to the induction of disease phenotype (Figure 7). Treatment with dexamethasone for 3 days, lowered the time spent by the fish at 37°C compared to the infected group (Table 6). However, the behavioral fever was distinctly dissimilar to the normal control group, suggesting that the symptoms of induction were still persistent even after 3 days treatment. When treated with DSV, the fish showed a dose-dependent reduction in the time spent at 37°C and a corresponding increase in the time spent at 29°C (Table 6). This is a very strong indication of rescue of behavioral fever with the test formulation within 3 days.

After 6 days of treatment with dexamethasone, the fish with the spike protein were observed to spend nearly equal time between the three different temperature chambers suggesting a reduction in the behavioral fever. The fish treated with the test formulation spent a majority of time in the 29°C chamber when compared to the 23 or 37°C chambers, showing a reversal of the behavioral fever seen in the infected fish. The time spent in each of the three temperature chambers by the 142 µg/kg treatment group was similar to that of the normal control fish (Table 6) suggesting a total reversal of the symptoms of induction with the recombinant spike protein.

Treatment with Divya-Swasari-Vati Enhances Survival After Induction of Disease Symptoms with the Recombinant Spike Protein of SARS-CoV-2

The survival of fish in all the seven groups was plotted against number of days after induction with the SARS-CoV-2 spike protein and starting the treatment with either dexamethasone or Divya-Swasari-Vati (DSV), as a

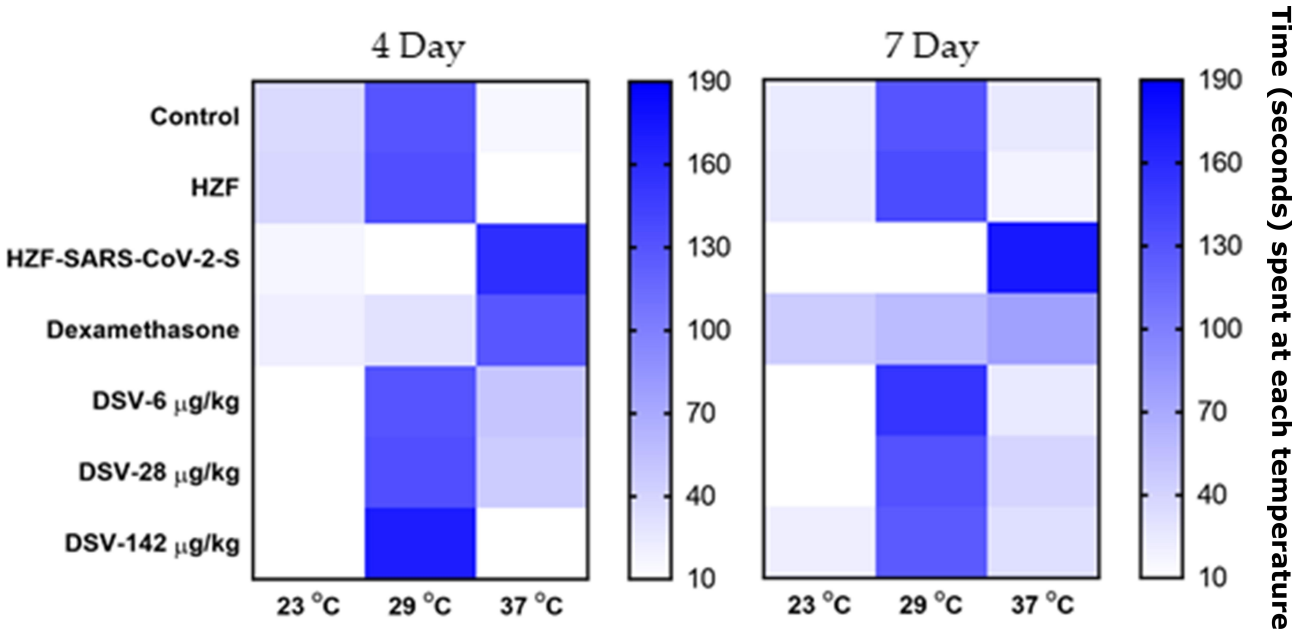

Figure 7 Heat map of behavioral fever. The time spent by individual fish in each temperature chamber is depicted as increased color intensity with an increase in the time spent. Data is presented as a mean of the observations.

Table 6 Behavioural Fever as a Reflection of the Body Temperature. Time Spent by Fish in Each of the Different Temperature Chambers is a Reflection of Their Body Temperature. A Single Fish Was Introduced to the 29°C Chamber, and the Time Spent in Each of the Temperature Chambers Was Measured. Results are Shown as Mean±SD for Each Group of Fish. # $P<0.0001$ When Compared to the Normal Control While * $P<0.0001$ When Compared to the Disease Control

Study Groups	4 Day Treatment			7 Day Treatment		
	23°C	29°C	37°C	23°C	29°C	37°C
Control	35.58±3.0	129.63±1.4	14.92±2.7	24.13±0.7	130.0±0.8	25.88±0.7
HZF	37.79±1.5	134.0±1.5	8.21±2.0	25.88±1.3	135.75±1.5	18.38±1.3
NZF-CoV-2-S	15.96#±1.6	7.04#±1.3	157.08#±1.6	2.38#±1.1	4.75#±1.3	172.88#±1.3
Dexamethasone	21.13*±2.3	30.46*±2.3	128.29*±1.9	45.54*±1.6	57.54*±2.0	76.92*±2.1
DSV-6 µg/kg	0*	129.75*±2.0	50.29*±2.0	3.54*±1.5	151.50*±1.9	25.0*±2.0
DSV-28 µg/kg	0*	133.96*±1.8	45.83*±1.8	9.04*±2.1	132.17*±2.2	38.79*±1.8
DSV-142 µg/kg	0*	170.0*±1.7	9.92*±1.8	22.29*±1.7	125.83*±2.1	31.88*±2.1

Kaplan–Meier Survival Curve. The normal control and A549 xenotransplanted fish had a 100% survival until day 10 when the study was terminated. The HZF-SARS-CoV2-S group had only 80% survival during the same time (Figure 8). Fish treated with a single dose of dexamethasone and three different dosages of DSV had 100% survival with no observed mortality, similar to the normal control group.

Divya-Swasari-Vati Ameliorates Cytokine Release in vivo and in vitro

Expression levels of the different cytokines IL-6, IL-10, and TNF-α were assessed by semi-quantitative RT-PCR. Total RNA was isolated from all the different groups of zebrafish and cDNA was reverse transcribed. The disease control fish showed a significant ($P<0.0001$) increase in the expression levels of all the three cytokine gene expression after 4 days and 7 days of the study period. Treatment with dexamethasone for 3 days and 6 days, decreased the expression significantly ($P<0.0001$), as shown in Figure 9. There was no significant reduction in IL-6 expression levels with 6 µg/kg Divya-Swasari-Vati after 3-day treatment but was significant ($P<0.001$) by 6 days. All the other treatments showed highly significant ($P<0.0001$) reduction in IL-6 gene expression levels. IL-10 levels were significantly down-regulated only with the highest dosage of Divya-Swasari-Vati (142 µg/kg) after 3 days and 6 days of treatment. Down-regulation of TNF-α was seen at significant levels ($P<0.0001$) only with

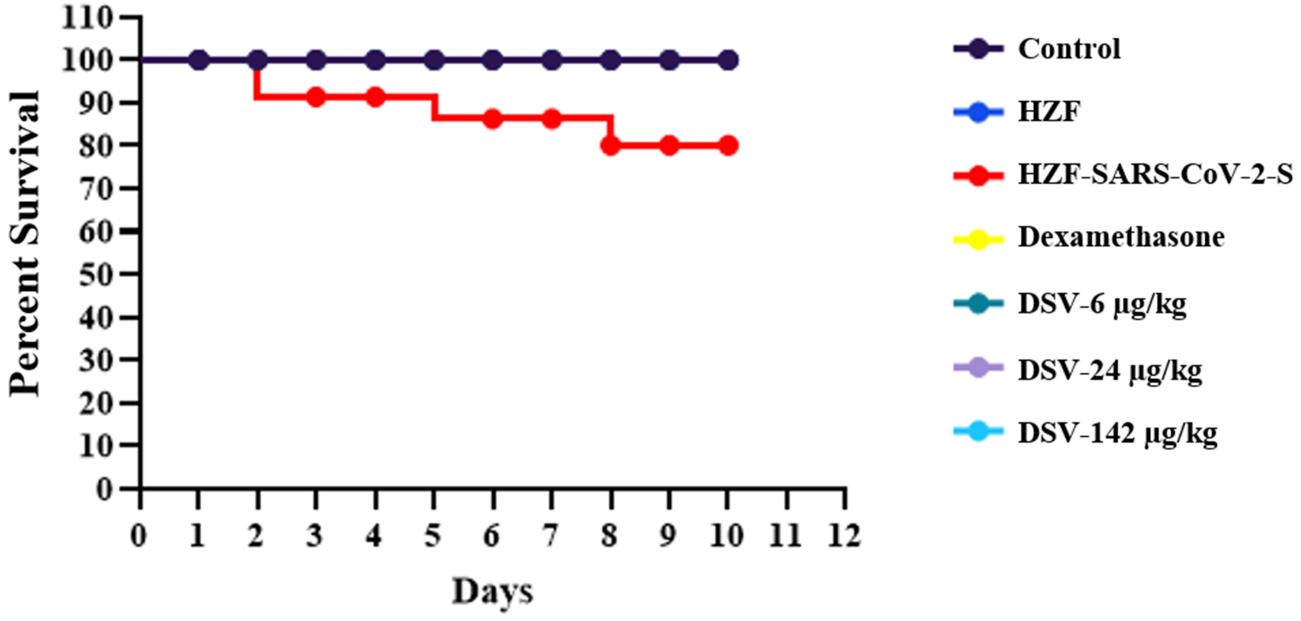

Figure 8 Survival analysis of the different groups of zebrafish presented as a Kaplan–Meier survival curve.

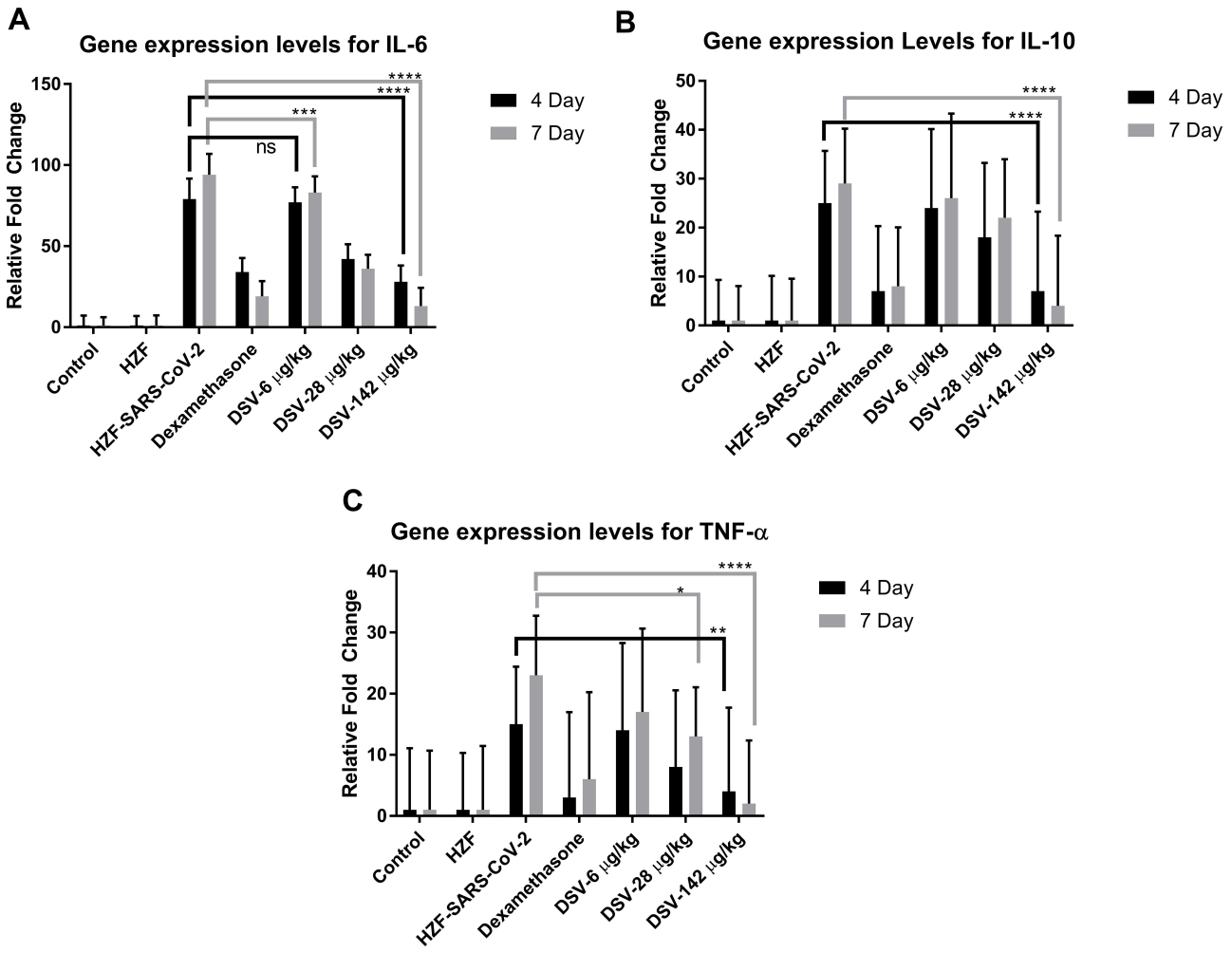

Figure 9 Gene expression levels of IL-6, IL-10, and TNF-α in vivo. (**A**) Dexamethasone and DSV at 28 µg/kg and 142 µg/kg showed highly significant (P<0.0001) reduction in the IL-6 expression levels while 6 µg/kg was significant at P<0.001. (**B**) IL-10 showed highly significant reduction with 142 µg/kg of DSV treatment and with dexamethasone, while the other dosages were not significant. (**C**) Dexamethasone showed significant (P<0.005) reduction of TNF-α levels at 4 days and P<0.0001 at 7 days. Divya-Swasari-Vati showed similar effects to the dexamethasone group, with 142 µg/kg dosage and only a slight reduction (P<0.05) with 28 µg/kg dosage after 7 days, rest of the treatments were not significant (ns). * P<0.05, ** P<0.05, *** P<0.001, **** P<0.0001.

142 µg/kg after 6 days of treatment but was only slightly significant (P<0.01) with 3 days of treatment.

In the A549 cells, under in vitro conditions, IL-1β induced secretory levels of IL-6 and TNF-α were determined by ELISA in the cell-culture supernatants. Pretreatment of the A549 cells with various concentrations of Divya-Swasari-Vati for a period of 24 hours had no effect on the viability of the cells. Simulation of the cytokine storm seen in SARS-CoV2 infection was mimicked by incubating the A549 cells for 24 hours in the presence of 500 pg/mL human IL-1β; and a significant increase in IL-6 and TNF-α release was observed when compared to untreated control (Figure 10). When the cells were co-incubated with different concentrations of DSV along with IL-1β, a dose-dependent reduction in the levels of both the cytokines were observed. This reduction was significant with 30 µg/mL and 100 µg/mL DSV, when compared to the cells that were stimulated with IL-1β but were untreated with the test formulation. There was no significant difference in the cytokine levels between 24 hours and 3-day treatment.

HPLC Analysis of the Phytocompounds Present in Divya-Swasari-Vati

Divya-Swasari-Vati formulation contained a number of different phytocompounds detected upon HPLC analysis. Gallic acid was the fastest eluate, as shown in Figure 11. Eugenol was the most abundant compound present in the DSV medicinal formulation followed by Piperine, Glycyrrhizin, and Gallic acid, as shown in Table 7.

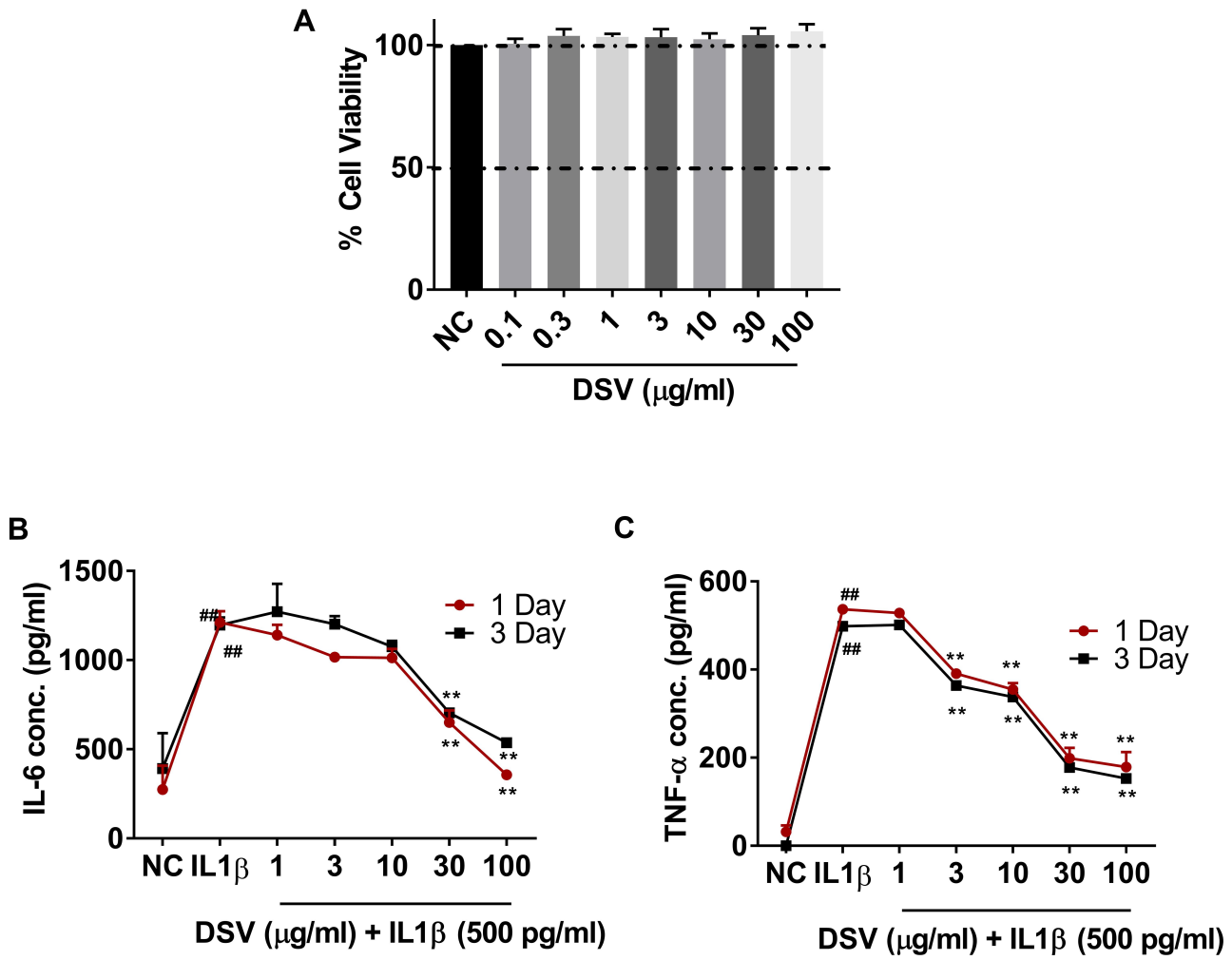

Figure 10 Release of IL-6 and TNF-α from human lung (A549) cells post stimulation with IL-1β in vitro. (**A**) Cell viability was estimated by Alamar blue assay during a 24-hour period. Results are expressed as mean±SD in triplicate analysis. (**B**) Cells were pre-treated with different concentration of DSV for either 1 day or 3 days before addition of IL-1β and DSV in the desired concentration. Cell supernatant was used in ELISA for the estimation of IL-6 expression 24 hours post-stimulation. Results are expressed as mean±SD in triplicate analysis. (**C**) Cell supernatant was used for TNF-α expression as above. Results are expressed as mean±SD ## $P<0.001$ when compared to the normal control (NC) and ** $P<0.01$ when compared with the IL-1β stimulated control without any test formulation treatments.

Discussion

The SARS-CoV-2 spike protein is a homo-trimer attached to the surface of the virion and is the primary point of contact with the ACE2 receptor on host cells. This interaction is the initial requirement for host cell recognition and entry that can lead to the establishment of a potent infection. Although not much is known about the susceptibility markers for this infection, genetic predisposition,[27] and a few risk factors such as several underlying conditions like diabetes, and hypertension may increase the risk.[28] Certain population groups may have a higher allele frequency for the ACE-2 gene and the susceptibility of this group may be different compared to other population groups under similar conditions.[29] Several variants have been identified in the ACE-2 protein that can alter the binding efficiency of the spike protein; however, these variations are rare and therefore may not have a wide population effect on reduction in viral infections.[30]

Previous studies with the SARS-CoV spike protein were shown to induce innate immune responses in human macrophages in vitro.[31] Similarly, the SARS-CoV-2 spike protein is being heralded as the ideal vaccine candidate due to previous studies in Hamster where it was shown to be highly immunogenic and protective against SARS-CoV challenge[32] and several virus neutralizing antibodies isolated from memory B cells from humans infected with SARS-CoV[33] and MERS-CoV.[34] A study published in July 2020 identified several epitopes on the spike protein of SARS-CoV-2 to be used as a multi-epitope vaccine against the virus.[35]

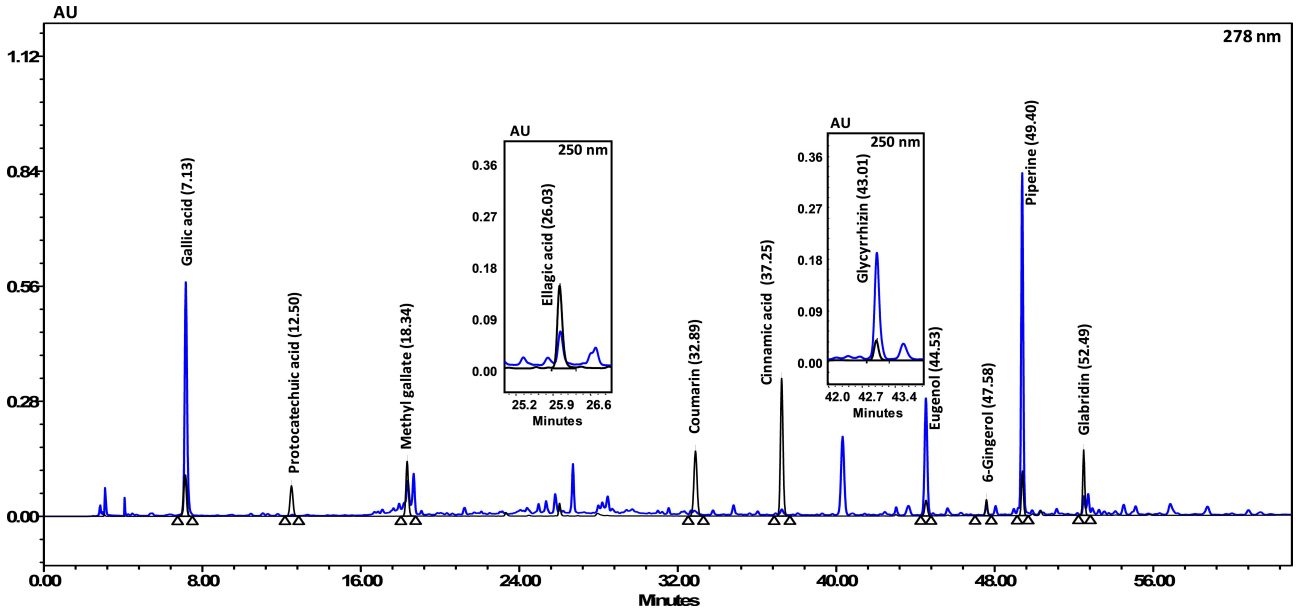

Figure 11 HPLC profile showing the different phyto-compounds identified in Divya-Swasari-Vati used in the present study. The quantified phytochemicals in DSV have been listed in Table 7

Due to the lack of a clear candidate drug for treatment of SARS-CoV-2 infection, several alternative methods of treatment including probiotics, aptamers, medicinal plants, and other natural compounds are being tried as either a cure or a preventive against the coronavirus.[36,37] Many of these, such as extracts of eucalyptus, and ginsenoside-Rb1, are being used either by themselves or in combination with prescribed anti-viral agents including Vitamin C, ritonavir, lopinavir, ribavirin, and others.[38]

In-silico docking studies by our group identified various phyto-compounds that can potentially reduce SARS-CoV-2 infection at multiple stages during the course of an infection, including Withanone and Tinocordiside.[39] Tinocordiside from *Tinospora cordifolia* reduced the free binding energy of the host cell ACE-2 and the SARS-CoV-2 spike protein's Receptor Binding Domain.[40] Other studies identified the potential use of several phyto-compounds such as diterpene, tetranortriterpenoid, phytosterols, and several other FDA approved compounds for efficient blocking of the major protease, Nsp9 replicase, and spike proteins of the SARS-CoV-2 virus.[41,42] The various bioactive compounds present in *Withania somnifera* (Ashwagandha), such as Withanone, Withanoside X, Ashwagandanolide, Dihydrowithaferin A, and Withanolide N were identified as potent inhibitors to the entry of the virus into the host cell using docking experiments in-silico.[39,43] Others have shown the stable binding of Withanoside V to the M^{pro} protease through dynamic simulations.[44]

In this study, we have used a calcium rich herbal formulation, Divya-Swasari-Vati, in a zebrafish xenograft model using A549 cells. The changes to the swim bladder, which is analogous to a human lung, morphology, and cytology was studied along with changes to the kidney due to the toxicity presented by the recombinant spike protein of SARS-CoV-2. Dexamethasone was used as a reference control as it is generally used as a high dose corticosteroid during the "Cytokine Storm" syndrome.[45,46] Divya-Swasari-Vati contains a mixture of different phytocompounds such as Gallic acid, Ellagic acid, Cinnamic acid, Eugenol, 6-Gingerol, Piperine, and Glycyrrhizin, as identified by HPLC. The formulation has been used for treatment of common cold, chronic cough, and other respiratory ailments in Indian Ayurveda. Glycyrrhizin has been shown to be the most active in inhibiting the replication of SARS-associated virus with very few side-effects.[47,48]

Many of the components of the Divya-Swasari-Vati medicinal formulation have been in use, In India, for the symptomatic treatment of common cold, asthma, and chronic cough. Essential oils from *P. integerrima* have been known to exert an anti-asthmatic activity due to their action on reducing TNF-α activity.[49,50] TNF-α has been implicated in several aspects of airway pathology including asthma[51] and retrospective analysis of plasma levels in cases of SARS-CoV-2, has shown increasingly higher levels of TNF-α with increasing severity of the infection.[52] Whole *Cressa cretica* plant is also known to

Table 7 Phytocompounds Present in Divya-Swasari-Vati Medicinal Formulation as Determined by HPLC (Figure 11). The Relative Abundance (w/w) of the Different Compounds are Shown. The Chemical Structures Shown Have Been Sourced from www.pubchem.com

Peak Number	Phytocompound	Structure	Retention Time (min)	Quantity (µg/mg)
1	Gallic acid	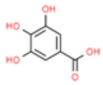	7.12	3.402
2	Protocatechuic acid		12.50	0.026
3	Methyl gallate		18.34	0.278
4	Ellagic acid	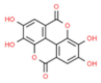	26.03	0.278
5	Coumarin		32.89	0.013
6	Cinnamic acid		37.25	0.030
7	Glycyrrhizin	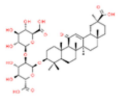	43.01	3.611
8	Eugenol		44.53	5.832
9	6-Gingerol	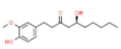	47.58	0.474

(*Continued*)

Table 7 (Continued).

Peak Number	Phytocompound	Structure	Retention Time (min)	Quantity (µg/mg)
10	Piperine	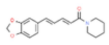	49.40	5.705
11	Glabridin	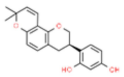	52.49	0.215

have broncho-dilatory activity, while the aerial parts contain many active compounds including coumarin derivatives and have anti-inflammatory and anti-oxidant activities.[53] The combination of airway dilation and anti-inflammatory properties may play a very important role in proper lung function, which is one of the major causes of death in SARS-CoV-2 infections.

Eugenol is the most abundant phenolic present in the essential oil of the dried flower bud of *Syzygium aromaticum* (clove) and is also found in the bark of cinnamon (*Cinnamomum zylancium*). Eugenol is known for its function as a free radical scavenger and an anti-inflammatory.[54,55] Cinnamon has been shown to suppress IL-1β, IL-6, and TNF-α activity in LPS-activated macrophages.[56] In this study, we observed increased infiltration of macrophages during disease phenotype induction after 3 days which was abolished by treatment with DSV. Methyl gallate is a phenolic acid that is prevalent in the plant kingdom and is quite often found in herbal remedies for its potent anti-inflammatory and anti-oxidant activities. In an experimental model of inflammation in arthritis, methyl gallate was shown to reduce neutrophil recruitment, and the production of mediators of inflammation, and macrophage activation.[57] The presence of such a wide range of anti-inflammatory compounds in the Divya-Swasari-Vati medicinal formulation could be seen in the drastic reduction in the numbers of infiltrating granulocytes in the treatment groups regardless of the dosages used.

The rhizome commonly called Ginger, *Zingiber officinale*, has been used for centuries as home remedy against common cold, asthma, and bronchitis. In modeling studies, a novel compound was identified, which has structural similarity to 6-gingerol and was found to have a strong binding affinity to the SARS-CoV-2 viral receptors.[58] These authors demonstrated strong binding affinity to a variety of targets including viral proteases, RNA binding protein, and Spike protein using molecular docking experiments. In addition to 6-gingerol, another group using computational approaches identified Piperidine and Piperanine from *Piper nigrum* and 8-Gingerol from ginger, to have a strong binding affinity to the SARS-CoV-2 particles.[59] Black pepper has been shown to exhibit endothelial barrier protective effects and suppressed leukocyte migration in vivo,[60] in a LPS induced inflammation model in mice. In our study the use of Divya-Swasari-Vati negated the hemorrhage observed by the induction of disease by the SARS-CoV-2 spike protein.

The use of several "Bhasma", the incinerated ash derived from various animal exo-skeleton or minerals treated with herbal decoctions, is unique to Ayurveda and is considered to be efficacious and non-toxic in nature. Bhasma are added to provide optimal alkalinity by neutralizing harmful acids in the body, as well as to provide easily absorbable and usable calcium to the body.[61] The mineral preparations have certain advantages over herbal formulations in that they are fast acting and effective in small doses. Divya-Swasari-Vati has seven different bhasma most of which have reported anti-inflammatory activity. Kapadrak Bhasma, Abhrak Bhasma, Godanti Bhasma, and Mukta-Shukti Bhasma, are calcium rich and are highly anti-inflammatory in nature.[49] Sphatika Bhasma is derived from calcined form of Alum and is known for its hemostatic and anti-inflammatory properties along with Tankan Bhasma (herbally processed ash from calcined borax), have been shown to have therapeutic efficacy in "disease of throat" and "disease of palate".[62] Praval pishti which is processed coral calcium, is used for the treatment of inflammation, cough due to phthisis, and several other ailments.[63] Several of the symptoms associated with

SARS-CoV-2 infection, are centered around inflammation and severe cytokine reactions. The various herbal and mineral components of Divya-Swasari-Vati, work as anti-inflammatory agents and could be highly beneficial in symptomatic reliefs.

Induction with the spike protein showed gross changes to the morphology of the swim bladder, analogous to that seen in human lung, most notably edema. The formation of an edematous gland within the bladder caused structural collapse which was not fully recovered with dexamethasone. This was also corroborated in the cytological examination where large amounts of cell debris were seen in the disease control air bladder, while the dexamethasone treatment group showed the presence of lymphocytes and macrophages in low numbers and slightly lower amount of cellular debris. Divya-Swasari-Vati treatment showed normal appearance of air bladder in size, shape, and color after 3 days. Longer presence of the spike protein for 7 days caused a collapse of the anterior lobe of the swim bladder which was not fully recovered in low and medium doses of the test formulation (6 µg/kg and 28 µg/kg) while a high dose (142 µg/kg) showed complete recovery. Over a 7-day period, the group treated with lower doses of DSV showed a moderate infiltration of granulocytes and elevated lymphocytes count. A substantial reduction of inflammatory cellular debris is clearly observed in the cytology indicating rescue morphology. The highest dosage used in the study, showed much higher lymphocyte count and a very low leukocyte count suggesting a marked reversal of the disease. A longer treatment showed normal epithelial cell and myocyte distribution along with a total lack of granulocytes in the cytology, suggesting that the inflammatory response to the disease has been ameliorated.

The gene expression levels of IL-6, IL-10, and TNF-α were measured in the study animals semi-quantitatively. The high dose of Divya-Swasari-Vati (142 µg/kg) showed highly significant reduction in the gene expression levels just after 3 days of treatment. The cytokine profile of the A549 cells that have been xenotransplanted in fish cannot be studied and, therefore, cells in culture were treated with IL-β and the effect of treatment with DSV was studied. A549 cells in culture showed an increased IL-6 and TNF-α secretion in the presence of IL-1β.

IL-6 upregulation has been linked to downregulation of ACE-2 and blocking the activity of this cytokine has already been used for managing hyper-inflammation in COVID-19 patients. Similarly, TNF-α has been shown to cause severe immune based pulmonary injury in COVID-19 patients.[64,65] In the current study, both IL-6 and TNF-α levels showed an increasing trend from day 4 to day 7 in the disease group and can be directly linked to the inflammatory pathology. However, this high level of the pro-inflammatory cytokines was significantly reduced upon treatment with Divya-Swasari-Vati. Together with the cytological identification of inflammation and recovery of the disease morphology when treated with DSV, we can conclude that the test formulation plays an important role in the reduction of the "Cytokine Storm" and promotes a healing immune response to the presence of the SARS-CoV-2 spike protein.

Untreated, SARS-CoV-2 infection has been known to cause multi-organ failure in about 11% of the patients.[66] In our study, we looked at the gross morphological and cytological changes to the kidney as a measure of organ failure. Induction of the disease phenotype with the recombinant spike protein caused a loss of tubular segments and vascular degeneration indicating renal necrosis, this was much more significant in a 7-day model compared to a 4-day model. The treatment with Divya-Swasari-Vati showed a kidney with packed network of mesonephros and highly pigmented melanocytes distributed throughout, suggesting a normal renal morphology. Cytological examination showed a dose-dependent reduction in the percentage of degenerative and necrotic cells compared to the HZF-SARS-CoV-2-S group. Treatment with the test formulation for a longer period in the presence of the spike protein showed a more gradual recovery of the kidney morphology. Lower doses did not rescue the disease morphology completely, with a high to moderate percentage of degenerative and necrotic cells, while a high dose (142 µg/kg), showed near normal kidney morphology with very low necrotic cells.

Another aspect of the SARS-CoV-2 infection is the loss of vascular integrity due to endothelial cell infection.-[67] In zebrafish this was seen as hemorrhagic regions on the skin in all the fish that were injected with the recombinant spike protein. Neither the dexamethasone treated nor the DSV treated fish had any hemorrhagic spots on the skin. This was also corroborated by the observation of behavioral fever. The normal control and the xenografted zebrafish spend more time in the 29°C chamber indicating normal body temperature, while the HZF-SARS-CoV-2-S group spent more time at 37°C indicating behavioral fever. Treatment with dexamethasone showed reduction in the behavioral fever reduction as the fish spent nearly equal

amount of time in the three temperature chambers. The Divya-Swasari-Vati treated group spent a majority of time in the 29°C chamber suggesting the rescue for high fever seen during the viral infection. Survival at the end of a 10-day period was determined and showed that only 80% of the fish survived when injected with the Spike protein of SARS-CoV-2 while the normal, xenotransplanted fish, and the treatment with dexamethasone, or with DSV had 100% survival.

Taken together these data suggest that induction of disease phenotype with SARS-CoV-2 spike protein induces several changes in the zebrafish that mirror the changes seen during the coronavirus infection. While dexamethasone alleviates most of the cytokine mediated immune responses, some of the morphological and cytological changes were not completely recovered. Treatment with Divya-Swasari-Vati for 7 days, not only changed the cytokine profile and associated immune cell infiltration, the morphological and cytological changes were completely reversed. All of the different phytocompounds identified in the DSV medicinal formulation have previously been shown to have potent anti-inflammatory effects. In our study, the infiltration of inflammatory immune cells was significantly reduced when treated with DSV for a period of 3 days. This change in immune cell profile when combined with the cytokine profile in A549 cells in vitro, suggest that the medicinal formulation Divya-Swasari-Vati, has potential anti-inflammatory effects in a SARS-CoV-2 spike protein-induced disease phenotype model in zebrafish.

Conclusion

In the present study, Divya-Swasari-Vati medicinal formulation was screened for therapeutic efficacy in a xenotransplanted zebrafish model for SARS-CoV-2 by injecting recombinant spike protein. The formulation showed moderate baseline rescue at lower doses (6 µg/kg and 28 µg/kg), and a complete recovery of preclinical end points such as renal degeneration and necrosis, improvement of behavioral fever, absence of skin hemorrhage, and survival rate at 142 µg/kg dose. The phytochemical rich formulation showed progressive recovery of immune cell infiltration with very few pro-inflammatory infiltrates at the end of the study period, suggesting it as an effective immunomodulator. The presented preclinical study shows the effectiveness of Divya-Swasari-Vati in reducing the inflammatory damage caused by SARS-CoV-2 spike protein; and detailed clinical investigations are recommended in human subjects of SARS-CoV-2 infection.

Acknowledgments

We appreciate the zebrafish test facilities and experimentations at our CRO partner, Pentagrit Labs, Chennai, India. We thank Dr Jyotish Shrivastava for phytochemical analysis. We extend our gratitude to Ms Priyanka Kandpal, Mr Tarun Rajput, Mr Gagan Kumar, and Mr Lalit Mohan for their swift administrative supports.

Funding

This research received no external funding. This presented work has been conducted using internal research funds from Patanjali Research Foundation Trust, Hardwar, India.

Disclosure

The authors declare no conflicts of interest for this work.

References

1. Zaman W, Saqib S, Ullah F, Ayaz A, Ye J. COVID -19: phylogenetic approaches may help in finding resources for natural cure. *Phytother Res*. 2020;ptr.6787. doi:10.1002/ptr.6787
2. Khan S, Ali A, Shi H, et al. COVID-19: clinical aspects and therapeutics responses. *Saudi Pharm J*. 2020;28(8):1004–1008. doi:10.1016/j.jsps.2020.06.022
3. Chhikara BS, Rathi B, Poonam JS. Corona virus SARS-CoV-2 disease COVID-19: infection, prevention and clinical advances of the prospective chemical drug therapeutics. *Chem Biol Lett*. 2020;7(1):63–72.
4. Thompson MR, Kaminski JJ, Kurt-Jones EA, Fitzgerald KA. Pattern recognition receptors and the innate immune response to viral infection. *Viruses*. 2011;3(6):920–940. doi:10.3390/v3060920
5. Shimizu M. Clinical Features of Cytokine Storm Syndrome. In: *Cytokine Storm Syndrome*. Springer International Publishing; 2019:31–41. doi:10.1007/978-3-030-22094-5_3
6. Grommes J, Soehnlein O. Contribution of neutrophils to acute lung injury. *Mol Med*. 2011;17(3–4):293–307. doi:10.2119/molmed.2010.00138
7. Chen N, Zhou M, Dong X, et al. Epidemiological and clinical characteristics of 99 cases of 2019 novel coronavirus pneumonia in Wuhan, China: a descriptive study. *Lancet*. 2020;395(10223):507–513. doi:10.1016/S0140-6736(20)30211-7
8. Huang C, Wang Y, Li X, et al. Clinical features of patients infected with 2019 novel coronavirus in Wuhan, China. *Lancet*. 2020;395(10223):497–506. doi:10.1016/S0140-6736(20)30183-5
9. Lai -C-C, Shih T-P, Ko W-C, Tang H-J, Hsueh P-R. Severe acute respiratory syndrome coronavirus 2 (SARS-CoV-2) and coronavirus disease-2019 (COVID-19): the epidemic and the challenges. *Int J Antimicrob Agents*. 2020;55(3):105924. doi:10.1016/j.ijantimicag.2020.105924
10. Mirzaie A, Halaji M, Dehkordi FS, Ranjbar R, Noorbazargan H. A narrative literature review on traditional medicine options for treatment of corona virus disease 2019 (COVID-19). *Complement Ther Clin Pract*. 2020;40:101214. doi:10.1016/j.ctcp.2020.101214
11. Lu H. Drug treatment options for the 2019-new coronavirus (2019-nCoV). *Biosci Trends*. 2020;14(1):69–71. doi:10.5582/bst.2020.01020
12. Benarba B, Pandiella A. Medicinal plants as sources of active molecules against COVID-19. *Front Pharmacol*. 2020;11. doi:10.3389/fphar.2020.01189.

13. Balkrishna A. *Ayurveda: Its Principles & Philosophies*. Divya prakashan; 2006.
14. Oreshkova N, Molenaar RJ, Vreman S, et al. SARS-CoV-2 infection in farmed minks, the Netherlands, April and May 2020. *Eurosurveillance*. 2020;25(23):23. doi:10.2807/1560-7917.ES.2020.25.23.2001005
15. Guo Q, Li M, Wang C, et al. Host and infectivity prediction of Wuhan 2019 novel coronavirus using deep learning algorithm. *bioRxiv*. 2020;2020. doi:10.1101/2020.01.21.914044
16. Johansen MD, Irving A, Montagutelli X, et al. Animal and translational models of SARS-CoV-2 infection and COVID-19. *Mucosal Immunol*. 2020;13(6):877–891. doi:10.1038/s41385-020-00340-z
17. Zhang Y, Liu H, Yao J, et al. Manipulating the air-filled zebrafish swim bladder as a neutrophilic inflammation model for acute lung injury. *Cell Death Dis*. 2016;7(11):e2470–e2470. doi:10.1038/cddis.2016.365
18. Palha N, Guivel-Benhassine F, Briolat V, et al. Real-time whole-body visualization of chikungunya virus infection and host interferon response in Zebrafish. Heise MT, ed. *PLoS Pathog*. 2013;9(9):e1003619. doi:10.1371/journal.ppat.1003619
19. Gabor KA, Goody MF, Mowel WK, et al. Influenza A virus infection in zebrafish recapitulates mammalian infection and sensitivity to anti-influenza drug treatment. *Dis Model Mech*. 2014;7(11):1227–1237. doi:10.1242/dmm.014746
20. Gomes MC, Mostowy S. The case for modeling human infection in Zebrafish. *Trends Microbiol*. 2020;28(1):10–18. doi:10.1016/j.tim.2019.08.005
21. Sepahi A, Kraus A, Casadei E, et al. Olfactory sensory neurons mediate ultrarapid antiviral immune responses in a TrkA-dependent manner. *Proc Natl Acad Sci*. 2019;116(25):12428–12436. doi:10.1073/pnas.1900083116
22. Shen W, Pu J, Sun J, et al. Zebrafish xenograft model of human lung cancer for studying the function of LINC00152 in cell proliferation and invasion. *Cancer Cell Int*. 2020;20(1):376. doi:10.1186/s12935-020-01460-z
23. Hamilton N, Sabroe I, Renshaw SA. A method for transplantation of human HSCs into zebrafish, to replace humanised murine transplantation models. *F1000Research*. 2018;7:594. doi:10.12688/f1000research.14507.2
24. Westerfield M. *The Zebrafish Book. A Guide for the Laboratory Use of Zebrafish (Danio Rerio)*. 4th ed ed. University of Oregon Press; 1993.
25. Li X, Huang L, Wu J, et al. Zebrafish xenograft model of human lung cancer for evaluating osimertinib resistance. *Biomed Res Int*. 2019;2019:1–10. doi:10.1155/2019/3129748
26. Coleman CM, Liu YV, Mu H, et al. Purified coronavirus spike protein nanoparticles induce coronavirus neutralizing antibodies in mice. *Vaccine*. 2014;32(26):3169–3174. doi:10.1016/j.vaccine.2014.04.016
27. Mohammadpour S, Torshizi Esfahani A, Halaji M, Lak M, Ranjbar R. An updated review of the association of host genetic factors with susceptibility and resistance to COVID-19. *J Cell Physiol*. 2020. doi:10.1002/jcp.29868
28. Halaji M, Farahani A, Ranjbar R, Heiat M, Dehkordi FS. Emerging coronaviruses: first SARS, second MERS and third SARS-CoV-2: epidemiological updates of COVID-19. *Le Infez Med*. 2020;28(\(suppl 1)):6–17.
29. Chen Y, Shan K, Qian W. Asians and Other Races Express Similar Levels of and Share the Same Genetic Polymorphisms of the SARS-CoV-2 Cell-Entry Receptor. 2020. doi:10.20944/PREPRINTS202002.0258.V1
30. Stawiski EW, Diwanji D, Suryamohan K, et al. Human ACE2 receptor polymorphisms predict SARS-CoV-2 susceptibility. *bioRxiv*. 2020;2020. doi:10.1101/2020.04.07.024752
31. Dosch SF, Mahajan SD, Collins AR. SARS coronavirus spike protein-induced innate immune response occurs via activation of the NF-κB pathway in human monocyte macrophages in vitro. *Virus Res*. 2009;142(1–2):19–27. doi:10.1016/j.virusres.2009.01.005
32. Buchholz UJ, Bukreyev A, Yang L, et al. Contributions of the structural proteins of severe acute respiratory syndrome coronavirus to protective immunity. *Proc Natl Acad Sci*. 2004;101(26):9804–9809. doi:10.1073/pnas.0403492101
33. Traggiai E, Becker S, Subbarao K, et al. An efficient method to make human monoclonal antibodies from memory B cells: potent neutralization of SARS coronavirus. *Nat Med*. 2004;10(8):871–875. doi:10.1038/nm1080
34. Corti D, Zhao J, Pedotti M, et al. Prophylactic and postexposure efficacy of a potent human monoclonal antibody against MERS coronavirus. *Proc Natl Acad Sci*. 2015;112(33):10473–10478. doi:10.1073/pnas.1510199112
35. Kar T, Narsaria U, Basak S, et al. A candidate multi-epitope vaccine against SARS-CoV-2. *Sci Rep*. 2020;10(1):10895. doi:10.1038/s41598-020-67749-1
36. Hasannejad-Bibalan M, Hekmatnezhad H. A light shining through darkness: probiotic against COVID-19. *J Curr Biomed Rep*. 2020;1(1).
37. Torabi R, Ranjbar R, Halaji M, Heiat M. Aptamers, the bivalent agents as probes and therapies for coronavirus infections: a systematic review. *Mol Cell Probes*. 2020;53:101636. doi:10.1016/j.mcp.2020.101636
38. Wu C-Y, Jan J-T, Ma S-H, et al. Small molecules targeting severe acute respiratory syndrome human coronavirus. *Proc Natl Acad Sci*. 2004;101(27):10012–10017. doi:10.1073/pnas.0403596101
39. Balkrishna A, Pokhrel S, Singh J, Varshney A. Withanone from Withania somnifera May Inhibit Novel Coronavirus (COVID-19) entry by disrupting interactions between viral s-protein receptor binding domain and host ACE2 receptor. *Virol J*. 2020;(preprint):1–26. doi:10.21203/rs.3.rs-17806/v1
40. Balkrishna A, Pokhrel S, Varshney A. Tinocordiside from Tinospora cordifolia (Giloy) May Curb SARS-CoV-2 Contagion by Disrupting the Electrostatic Interactions between Host ACE2 and Viral S-Protein Receptor Binding Domain. *Comb Chem High Throughput Screen*. 2020;23. doi:10.2174/1386207323666201110152615
41. Chandel V, Sharma PP, Raj S, Choudhari R, Rathi B, Kumar D. Structure-based drug repurposing for targeting Nsp9 replicase and spike proteins of severe acute respiratory syndrome coronavirus 2. *J Biomol Struct Dyn*. 2020;1–14. doi:10.1080/07391102.2020.1811773
42. Chandel V, Raj S, Rathi B, Kumar D. In silico identification of potent FDA approved drugs against Coronavirus COVID-19 main protease: a drug repurposing approach. *Chem Biol Lett*. 2020;7(3):166–175.
43. Chikhale RV, Gurav SS, Patil RB, et al. Sars-cov-2 host entry and replication inhibitors from Indian ginseng: an in-silico approach. *J Biomol Struct Dyn*. 2020:1–12. doi:10.1080/07391102.2020.1778539.
44. Tripathi MK, Singh P, Sharma S, Singh TP, Ethayathulla AS, Kaur P. Identification of bioactive molecule from Withania somnifera (Ashwagandha) as SARS-CoV-2 main protease inhibitor. *J Biomol Struct Dyn*. 2020;1–14. doi:10.1080/07391102.2020.1790425
45. Saghazadeh A, Rezaei N. Towards treatment planning of COVID-19: rationale and hypothesis for the use of multiple immunosuppressive agents: anti-antibodies, immunoglobulins, and corticosteroids. *Int Immunopharmacol*. 2020;84:106560. doi:10.1016/j.intimp.2020.106560
46. Felsenstein S, Herbert JA, McNamara PS, Hedrich CM. COVID-19: immunology and treatment options. *Clin Immunol*. 2020;215:108448. doi:10.1016/j.clim.2020.108448
47. Chen F, Chan K, Jiang Y, et al. In vitro susceptibility of 10 clinical isolates of SARS coronavirus to selected antiviral compounds. *J Clin Virol*. 2004;31(1):69–75. doi:10.1016/j.jcv.2004.03.003
48. Cinatl J, Morgenstern B, Bauer G, Chandra P, Rabenau H, Doerr H. Glycyrrhizin, an active component of liquorice roots, and replication of SARS-associated coronavirus. *Lancet*. 2003;361(9374):2045–2046. doi:10.1016/S0140-6736(03)13615-X

49. Balkrishna A, Solleti SK, Singh H, Tomer M, Sharma N, Varshney A. Calcio-herbal formulation, Divya-Swasari-Ras, alleviates chronic inflammation and suppresses airway remodelling in mouse model of allergic asthma by modulating pro-inflammatory cytokine response. *Biomed Pharmacother*. 2020;126:110063. doi:10.1016/j.biopha.2020.110063
50. Rana S, Shahzad M, Shabbir A. Pistacia integerrima ameliorates airway inflammation by attenuation of TNF-α, IL-4, and IL-5 expression levels, and pulmonary edema by elevation of AQP1 and AQP5 expression levels in mouse model of ovalbumin-induced allergic asthma. *Phytomedicine*. 2016;23(8):838–845. doi:10.1016/j.phymed.2016.04.006
51. Brightling C, Berry M, Amrani Y. Targeting TNF-α: a novel therapeutic approach for asthma. *J Allergy Clin Immunol*. 2008;121(1):5–10. doi:10.1016/j.jaci.2007.10.028
52. Qin C, Zhou L, Hu Z, et al. Dysregulation of immune response in patients with coronavirus 2019 (COVID-19) in Wuhan, China. *Clin Infect Dis*. 2020;71(15):762–768. doi:10.1093/cid/ciaa248
53. Sunita P, Jha S, Pattanayak S. In-vivo antitussive activity of *cressa cretica Linn*. using Cough Model in Rodents. *Pharmacognosy Res*. 2009;1(3):157–161.
54. Barboza JN, da Silva Maia Bezerra Filho C, Silva RO, Medeiros JVR, de Sousa DP. An overview on the anti-inflammatory potential and antioxidant profile of Eugenol. *Oxid Med Cell Longev*. 2018;2018:1–9. doi:10.1155/2018/3957262
55. Chericoni S, Prieto JM, Iacopini P, Cioni P, Morelli I. In vitro activity of the essential oil of Cinnamomum zeylanicum and Eugenol in peroxynitrite-induced oxidative processes. *J Agric Food Chem*. 2005;53(12):4762–4765. doi:10.1021/jf050183e
56. Kim ME, Na JY, Lee JS. Anti-inflammatory effects of trans-cinnamaldehyde on lipopolysaccharide-stimulated macrophage activation via MAPKs pathway regulation. *Immunopharmacol Immunotoxicol*. 2018;40(3):219–224. doi:10.1080/08923973.2018.1424902
57. Correa LB, Pádua TA, Seito LN, et al. Anti-inflammatory effect of methyl gallate on experimental arthritis: inhibition of neutrophil recruitment, production of inflammatory mediators, and activation of macrophages. *J Nat Prod*. 2016;79(6):1554–1566. doi:10.1021/acs.jnatprod.5b01115
58. Rathinavel T, Palanisamy M, Palanisamy S, Subramanian A, Thangaswamy S. Phytochemical 6-Gingerol – a promising Drug of choice for COVID-19. *Int J Adv Sci Eng*. 2020;06(04):1482–1489. doi:10.29294/IJASE.6.4.2020.1482-1489
59. Rajagopal K, Byran G, Jupudi S, Vadivelan R. Activity of phytochemical constituents of black pepper, ginger, and garlic against coronavirus (COVID-19): an *in silico* approach. *Int J Heal Allied Sci*. 2020;9(5):43–50. doi:10.4103/ijhas.IJHAS_55_20
60. Lee W, Yoo H, Kim JA, et al. Barrier protective effects of piperlonguminine in LPS-induced inflammation in vitro and in vivo. *Food Chem Toxicol*. 2013;58:149–157. doi:10.1016/j.fct.2013.04.027
61. Pal D, Sahu C, Haldar A. Bhasma: the ancient Indian nanomedicine. *J Adv Pharm Technol Res*. 2014;5(1):4. doi:10.4103/2231-4040.126980
62. Sahoo I, More SS, Jadhav V, Dalai S, Sahoo M. Clinical appraisal on therapeutic efficacy of tankana & sphatika bhasma with madhu pratisarana in Tundikeri. *J Drug Deliv Ther*. 2019;9(6):130–134. doi:10.22270/jddt.v9i6.3707
63. Mishra A, Mishra AK, Tiwari OP, Jha S. In-house preparation and characterization of an Ayurvedic bhasma: praval bhasma. *J Integr Med*. 2014;12(1):52–58. doi:10.1016/S2095-4964(14)60005-4
64. Gubernatorova EO, Gorshkova EA, Polinova AI, Drutskaya MS. IL-6: relevance for immunopathology of SARS-CoV-2. *Cytokine Growth Factor Rev*. 2020;53:13–24. doi:10.1016/j.cytogfr.2020.05.009
65. Mehta P, McAuley DF, Brown M, Sanchez E, Tattersall RS, Manson JJ. COVID-19: consider cytokine storm syndromes and immunosuppression. *Lancet*. 2020;395(10229):1033–1034. doi:10.1016/S0140-6736(20)30628-0
66. Chen J, Qi T, Liu L, et al. Clinical progression of patients with COVID-19 in Shanghai, China. *J Infect*. 2020;80(5):e1–e6. doi:10.1016/j.jinf.2020.03.004
67. Varga Z, Flammer AJ, Steiger P, et al. Endothelial cell infection and endotheliitis in COVID-19. *Lancet*. 2020;395(10234):1417–1418. doi:10.1016/S0140-6736(20)30937-5